T.C.
DOKUZ EYLUL UNIVERSITY
IZMIR INTERNATIONAL BIOMEDICINE AND GENOME INSTITUTE

IN VIVO INVESTIGATION OF THE EPIGENETIC FUNCTIONS OF THE CENP-A AMINO TERMINAL

TUĞBA ŞEHİTOĞULLARI

MOLECULAR BIOLOGY AND GENETICS MASTER'S PROGRAM

MASTER OF SCIENCE THESIS

İZMİR-2022

THESIS CODE: DEU.HSI.MSc- 2020850023

T.C.
DOKUZ EYLUL UNIVERSITY
IZMIR INTERNATIONAL BIOMEDICINE AND GENOME INSTITUTE

IN VIVO INVESTIGATION OF THE EPIGENETIC FUNCTIONS OF THE CENP-A AMINO TERMINAL

MOLECULAR BIOLOGY AND GENETICS MASTER'S PROGRAM

MASTER OF SCIENCE THESIS

TUĞBA ŞEHİTOĞULLARI

Supervising Faculty Member: Assoc. Prof. M. Kasım DİRİL

TEZ KODU: DEU.HSI.MSc- 2020850023

Dokuz Eylül University İzmir International Biomedicine and Genome Institute Department of Genomics and Molecular Biotechnology, Molecular Biology and Genetics Graduate Program Master of Science student with no 2020850023, Tuğba ŞEHİTOĞULLARI has successfully completed her Master of Science thesis titled '' In vivo Investigation of the Epigenetic Functions of the CENP-A Amino Terminal'' on the date of June 30, 2022.

CHAIR
Assoc Prof. M. Kasım DİRİL
İzmir International Biomedicine and Genome Institute
Department of Genomics and Molecular Biotechnology

MEMBER
Assoc Prof. Şerif ŞENTÜRK
İzmir International Biomedicine and Genome Institute
Department of Genomics and Molecular Biotechnology

MEMBER
Prof. Dr. Abdullah YALÇIN
Aydin Adnan Menderes University
Department of Medical Biology

SUBSTITUTE MEMBER
Prof.Dr. Gizem DÖNMEZ YALÇIN
Aydin Adnan Menderes University
Department of Medical Biology

SUBSTITUTE MEMBER
Dr. Hani ALOTAİBİ
İzmir International Biomedicine
and Genome Institute
Department of Biomedicine and
Health Technologies

Dokuz Eylül Üniversitesi İzmir Uluslararası Biyotıp ve Genom Enstitüsü, Genom Bilimleri ve Moleküler Biyoloji Anabilim Dalı, Moleküler Biyoloji ve Genetik Yüksek Lisans Programı 2020850023 numaralı öğrencisi Tuğba ŞEHİTOĞULLARI'nın ''CENP-A Amino Terminalinin Epigenetik Fonksiyonlarının in vivo Araştırılması" konulu Yüksek Lisans tezi 30.06.2022 tarihinde yapılan savunma sınavı sonucunda başarılı olmuştur.

BAŞKAN
Doç. Dr. M. Kasım DİRİL
İzmir Uluslararası Biyotıp ve Genom Enstitüsü
Genom Bilimleri ve Moleküler Biyoteknoloji Anabilim Dalı

JÜRİ ÜYESİ
Doç.Dr. Şerif ŞENTÜRK
İzmir Uluslararası Biyotıp ve Genom Enstitüsü.
Genom Bilimleri ve Moleküler Biyoteknoloji
Anabilim Dalı

JÜRİ ÜYESİ
Prof.Dr. Abdullah YALÇIN
Aydin Adnan Menderes Üniversitesi
Tibbi Biyoloji Anabilim Dali

YEDEK ÜYE
Prof.Dr. Gizem DÖNMEZ YALÇIN
Aydin Adnan Menderes Üniversitesi
Tibbi Biyoloji Anabilim Dali

YEDEK ÜYE
Dr. Öğr.Üyesi Hani Alotaibi
İzmir Uluslararası Biyotıp ve Genom Enstitüsü.
Biyotip ve Sağlik Teknolojileri Anabilim Dalı

TABLE OF CONTENTS

INDEX OF TABLES

INDEX OF FIGURES

LIST OF ABBREVIATIONS

BSA	Bovine serum albumin
CENP-A	Centromeric Protein A
CO2	Carbon dioxide
CRISPR	Clustered Regularly Interspaced Short Palindromic Repeats
CRISPR-EZ	Ribonucleoprotein electroporation of zygotes
ddH2O	Distilled Deionized water
DNA	Deoxyribose nucleic acid
EtOH	Ethanol
HEPES	4-(2-hydroxyethyl)-1-piperazineethanesulfonic acid
hCG	Human chorionic gonadotropin
HDR	Homology-directed repair
IU	International unit
IVT	In vitro transcription
MEF	Mouse embryonic fibroblasts
NHEJ	Non-homologous end-joining repair
Opti-MEM	Reduced-Serum Medium
PAM	Protospacer adjacent motif
PMSG	Pregnant mare serum gonadotropin
PTMs	Post-translational modifications
PCR	Polymerase Chain Reaction
RNA	Ribonucleic acid
RNP	Ribonucleoprotein
sgRNA	short guide RNA
S7p	Serin 7 phosphorylation
Tyr	Tyrosinase
WT	Wild Type

ACKNOWLEDGEMENT

I'd like to express my gratitude to Stefan Dimitrov and Kasım Diril for their encouragement and academic leadership during my master's degree. Without their expertise and direction, it is impossible to get to a successful conclusion. I am grateful for all the lessons, discussions, and guidance that they provided.

I am grateful to Kerem Esmen for all of the work he did in animal research and for the excellent education and friendship he provided. I thank Imtiaz Nisar Lone for his instruction and molecular biology teachings throughout my master's degree.

I would like to thank my lovely lab mates and IBG family; Ceren Şahin, Esin Özkuru, Şeyma Yıldız, Esra Türker, Abed Alkerem, Soheil Akbari, Vedat Sarı, Sude Uyulgan, Ayşenur Öner, Gizem Öztürk, Burcu Şengez for their friendship, support, and encouragement. Your amazing friendship made İzmir feel like home to me.

I am truly thankful to my dear family for their unconditional love and support, as well as for always having my back. Thank you to my grandmother, Meryem Şengil, for her uplifting phone calls and prayers whenever I felt down.

Thank you all.

.

In vivo Investigation of the Epigenetic Functions of the CENP-A Amino Terminal

Tuğba Şehitoğulları

İzmir International Biomedicine and Genome Institute
Dokuz Eylül University Sağlık Yerleşkesi
Balçova 35340 İzmir/TURKEY

ABSTRACT

Centromeric Protein A (CENP-A) is a histone H3 variant. During mitosis, it drives kinetochore formation with other centromere-specific DNA binding proteins. Furthermore, CENP-A serves as an epigenetic marker that determines the identification of centromeres. Phosphorylation of the CENP-A N-terminal has drawn a lot of attention since it differs greatly from other H3 variants. Phosphorylation of human CENP-A serine 7 (S7p) is of particular interest because it resembles H3 S10p, a marker of mitotic entry. There are conflicting findings related to the purpose of S7 phosphorylation during cell division. Besides the lack of consensus on human CENP-A S7 phosphorylation, the function of corresponding phosphorylation sites in other species needs to be investigated. In a recent publication, the first three serines (S15, S16, and S22) of the murine CENP-A were proposed to be phosphorylation sites with an analogous role to human CENP-A S7p during mitosis. However, no *in vivo* study has been reported addressing S15 and S16 functions. In order to understand the purpose of murine CENP-A N-terminal phosphorylation, we decided to create a knockin mouse model expressing S15A and S16A non-phosphorylatable residue substitutions. We used CRISPR-EZ technology (CRISPR ribonucleoprotein Electroporation of Zygotes) to genetically engineer mice. Firstly, we edited the mouse *Tyr* locus which has published targeting and genotyping protocols, in order to try and establish our own protocols. After successfully deriving the albino Tyr knock-out mouse model, we moved forward to create the CENP-A knockin mouse model. Homozygous knockin mice were viable and fertile suggesting that CENP-A N-terminal phosphorylation does not have a crucial role for chromosome segregation. Detailed studies will need to be carried out to characterize more subtle epigenetic functions of N-terminal phosphorylation.

Keywords: CENP-A, CRISPR-EZ, knockin mouse models

CENP-A Amino Terminalinin Epigenetik Fonksiyonlarının *In vivo* Araştırılması

Tuğba Şehitoğulları

İzmir Uluslararası Biyotıp ve Genom Enstitüsü
Dokuz Eylül University Sağlık Yerleşkesi
Balçova 35340 İzmir/TURKEY

ÖZET

Sentromerik Protein A (CENP-A) bir histon H3 varyantıdır. Diğer sentromere özgü DNA bağlayıcı faktörlerle birlikte mitoz sırasında kinetokor düzeneğini yönlendirir. Ayrıca, CENP-A, sentromerlerin tanımlanmasını belirleyen epigenetik bir belirteç görevi görür. CENP-A N-terminalinin fosforilasyonu, diğer H3 varyantlarından farklı olduğu için araştırmacıların ilgi odağı olmuştur. İnsan CENP-A serin 7'nin (S7p) fosforilasyonu mitotik girişin bir belirteci olan H3 S10p'ye benzerliği sebebiyle özellikle ilgi çekicidir. Hücre bölünmesi sırasında S7 fosforilasyonunun fonksiyonu ile ilgili tartışmalı bulgular yayınlanmıştır. İnsan CENP-A S7 fosforilasyonu konusunda fikir birliği olmamasının yanı sıra, diğer türlerde karşılık gelen fosforilasyon bölgelerinin işlevi araştırılması gerekeklidir. Yakın tarihli bir yayında, murin CENP-A'nın ilk üç serininin (S15, S16 ve S22) mitoz sırasında insan CENP-A S7p'ye benzer bir rolü olan fosforilasyon bölgeleri olduğu öne sürülmüştür. Bununla birlikte, S15 ve S16 fonksiyonlarını ele alan *in vivo* bir çalışma bildirilmemiştir. Fare CENP-A N-terminal fosforilasyonunun amacını anlamak için, S15A ve S16A fosforile edilemeyen rezidüleri ifade eden bir knockin fare modeli oluşturmayı amaçladık. Farelerin genetik mühendisliğini yapmak için CRISPR-EZ teknolojisini (Zigotların CRISPR ribonükleoprotein Elektroporasyonu) kullandık. İlk olarak, kendi protokollerimizi optimize etmek için, hedefleme ve genotipleme protokolleri yayınlanan fare Tyr lokusunu düzenledik. Albino Tyr knockout fare modelini başarıyla ürettikten sonra, CENP-A knockout fare modelini oluşturmayı hedefledik. Oluşturulan homozigot knockin fareleri canlı ve doğurgan olması sebebiyle CENP-A N-terminal fosforilasyonunun kromozom ayrımı için önemli bir rolü olmadığı sonucuna vardık. N-terminal fosforilasyonunun epigenetik fonksiyonlarını karakterize etmek için ayrıntılı çalışmaların yapılması gerekmektedir.

Anahtar Sözcükler: CENP-A, CRISPR-EZ, knockin fare modelleri

1. INTRODUCTION AND AIM

It's proven that CENP-A plays an important role during mitosis and meiosis with the arranging of chromosome segregation. To gain detailed knowledge we should examine the role of post-translational modifications (PTMs) during the cell cycle. Previous studies on human CENP-A S7p, revealed contradictory data related to its role in mitosis. Multiple studies demonstrated that S7p had no influence on chromosomal alignment, fusion, or separation (Barra et al. 2019; Zeitlin et al., 2001). On the other hand, blocking phosphorylation of CENP-A S7 has been shown to cause prometaphase delay and chromosome misalignment defects. (Goutte-Gattat et al., 2013; Kunitoku et al., 2003). In light of this information, the question arises whether the findings on the mitotic role of human CENP-A phosphorylation can be generalized or only applicable to human cells. According to the literature, serines 15 and 16 found in mouse CENP-A N-Terminal, are believed to function like human CENP-A S7p as crucial PTM sites for mitosis in terms of centromere integrity.

The primary goal of this study is to elucidate the roles of serine 15 and 16 phosphorylations by developing a knockin mouse model. Since there was no in-vivo research found on this issue, creating a mouse model will be a more precise way to study the effects of CENP-A S15 and S16 and will make it possible to conduct a comprehensive epigenetic study. To achieve this goal, a high-efficiency embryo and mouse editing method based on RNP electroporation, embryo culture and transfer has been selected. To evaluate dependent and independent factors while developing an in vivo model, we decided to use the CRISPR-EZ technique, starting with published Tyr-gene editing strategies (Modzelewski et al., 2018). Compared to other in-vivo gene editing techniques including microinjection-based technology, CRISPR-EZ has the highest editing efficiency and reliability. After successfully developing a Tyr-knock out mice with an albino coat color phenotype, the same strategy was used to create the CENP-A S15A; S16A knockin mice.

2. GENERAL INFORMATION

2.1 Chromatin Structure and Organization

In eukaryotes, the genomic material is arranged with chromosomes. In the cells, this arrangement provided deoxyribonucleic acid (DNA) and proteins called histones together they formed chromatin. Basically, chromatin is the complex formed by both DNA and related proteins. DNA and histone proteins are equally distributed in the chromatin structure. From an organizational perspective, chromatin plays a very essential role in packaging almost 2m of DNA into a more compact structure (Lee & Orr-Weaver, 2001). Chromatin is composed of small core repetitive functional units called nucleosomes. Each nucleosome contains eight histone proteins wrapped around 146bp DNA (Hall et al., 2020). According to previous in vitro studies, high-order organizations of chromatin define in 10nm and 30nm long fiber scales configurations. 10nm scales of chromatin architecture known as ‘’beads on string’’ which include tightly packaged histones wrapped into DNA (Figure 1) (Woodcock and Dimitrov,2001).

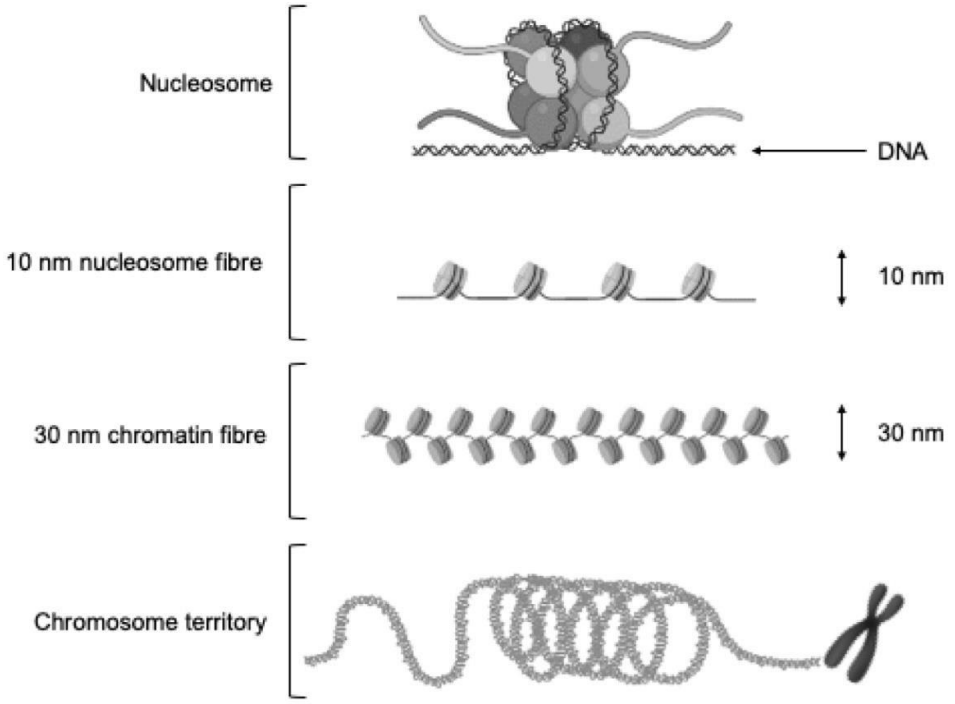

Figure 1. Representation of chromatin packaging into high-order organizations. The most leisure state is the nucleosome filament combined with DNA. 10nm scale of chromatin is defined

as ‘’beads on a string’’ then resembled chromatin’s second structure which is a 30nm fiber state. In the final state, condensation fibers and histones form chromosome territory (adapted from Hall et al., 2020).

2.1.1 Heterochromatin and Euchromatin

The chromatins of eukaryotic organisms are typically categorized into two heterochromatin and euchromatin. Heterochromatin is composed of inactive or dense chromatin regions, and its percentage in total chromatin ranges from %10 to 25, based on the individual's age, the type of cell, and the species. Heterochromatin is classified into two types as constitutive and facultative. During the course of a cell's life, constitutive heterochromatin refers to the chromatin regions that remain transcriptionally inactive. Facultative heterochromatin is an area of euchromatin that can be transcriptionally active when needed (Allshire & Madhani, 2017).

2.2 Histones

Histones are the core protein component of chromatin which is found as an alkaline feature that allows the binding of negatively charged DNA strands. These basic biochemical characteristics of histones are provided by their abundance of lysine and arginine amino acids. Their mass is found at approximately ∼15KD. Histones are divided into five subgroups according to their contribution to chromosome arrangement. H2A, H2B, H3, and H4 are known as core histones, whereas histone H1 is considered to be a linker histone. At the nucleosome core, histones are found in two copies which formed an octameric structure. The linker histone protein H1 is connected with the nucleosome cores. Core histone proteins are highly conserved compared to linker histones. Linker histones are rich in lysine residues, and they do not have a histone-fold motif (Figure2) (Mariño-Ramírez et al., 2005).

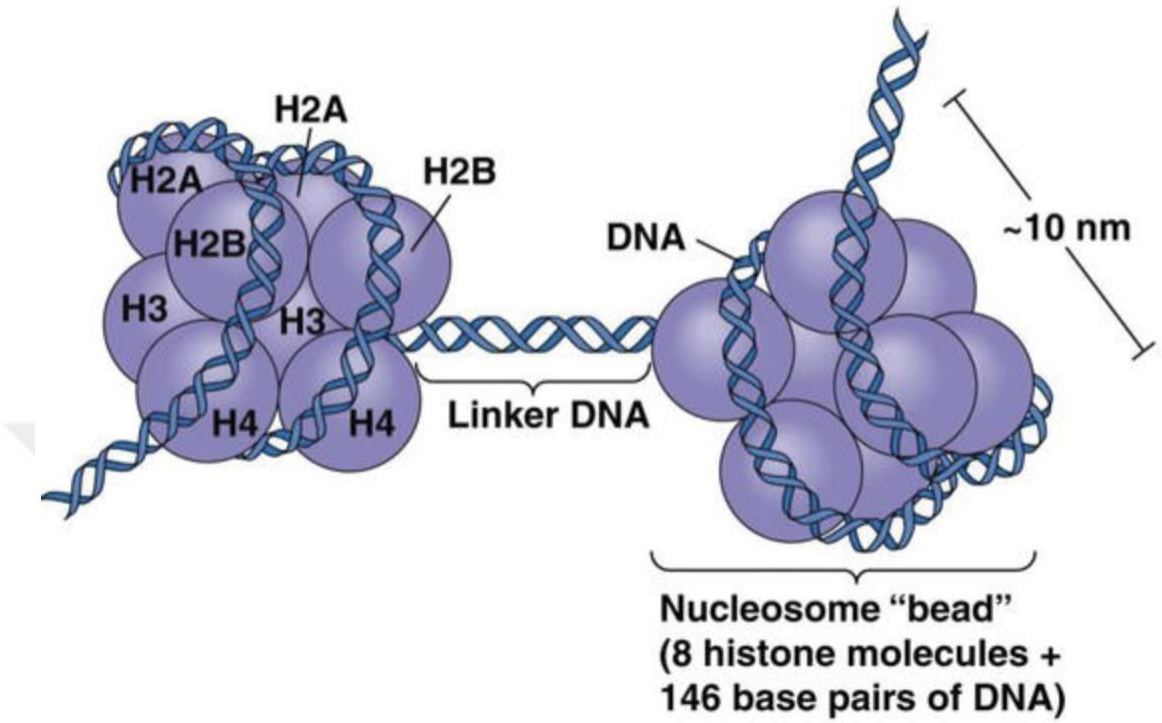

Figure 2. Schematic demonstration of the nucleosome structure. The nucleosome core includes couples of histone octamer H2A, H2B, H3, and H4. The DNA double helix is rolled up approximately ~1.7 times the histone octamer (adapted from Caputi et al., 2017).

2.2.1 Histone Posttranslational Modifications

Histones are served as hubs for many PTMs because of their versatility in the context of structure and association with double-helix DNA. PTMs are covalent arrangements between histones and DNA strands that include phosphorylation, methylation, acetylation, ubiquitylation, ADP-ribosylation, SUMOylation, and glycosylation. PTM serves a critical role in many cellular events such as gene expression, regulation, chromosome packaging, epigenetic imprinting, DNA damage, and DNA repair (Ramazi et al., 2020). PTM acts as a chromatin remodeler which is closely associated with the ‘’histone code’’ hypothesis. According to the hypothesis, in a general manner, PTMs are a major part that controls the transcription process. Another key point suggested by the hypothesis is that PTMs dominate gene expression via recruiting proteins recognized by protein domains found in histone docking sites (Strahl and Allis,2000). Furthermore, PTMs are related to

the occurrence of many diseases including cancer, neurodegenerative and developmental problems, and heart failure.

2.2.2 Histone phosphorylation

Histone phosphorylation is the process of adding phosphate groups into serine, threonine, and tyrosine residue operated by kinases. By using phosphatases, this process could be reversed with a hydrolysis event (Rossetto et al., 2012). Phosphorylation is a very effective tool in terms of regulating cellular events in a rapid manner. In the literature, the well-known example related to phosphorylation of serine residue 139 in H2A(X) which is one of the H2A variants. (Sharma et al., 2012). This phosphorylation act as a signal for starting the DNA damage and repair process.
There are various studies that revealed the importance of histone phosphorylation in chromatin chromatin regulation and other nuclear processes.

2.3 Histone Variants

Histone variants, non-allelic isoforms paralogs of common histones, are available to carry out activities throughout the cell cycle and accumulate in post-mitotic cells, while bulk histones are only deposited in S-phase (Talbert & Henikoff, 2021). There have been identified numerous histone variants related to H2A, H2B, H3, and H1 while H4 does not have histone variant.
Histone variant's expression shows diversity in terms of tissue-specificity, cell cycle, and developmental processes. Histone variants mostly share sequence similarities with the conventional histones' protein terminals.

2.3.1 H3 Variants

Five H3 variants have been detected in mammals: two canonical versions H3, H3.2, and the mammalian-specific H3.1, and H3.3 the centromere-specific variant also named CENP-A, and the testis-specific histone H3t. Only a few amino acid sites separate the replacement variant H3.3 from its canonical equivalents. H3.3 and the canonical H3 variant have separate nucleosome assembly mechanisms through interactions with particular histone chaperones, although it is unclear if these amino acid changes are sufficient to drive these processes. (Szenker et al., 2011)

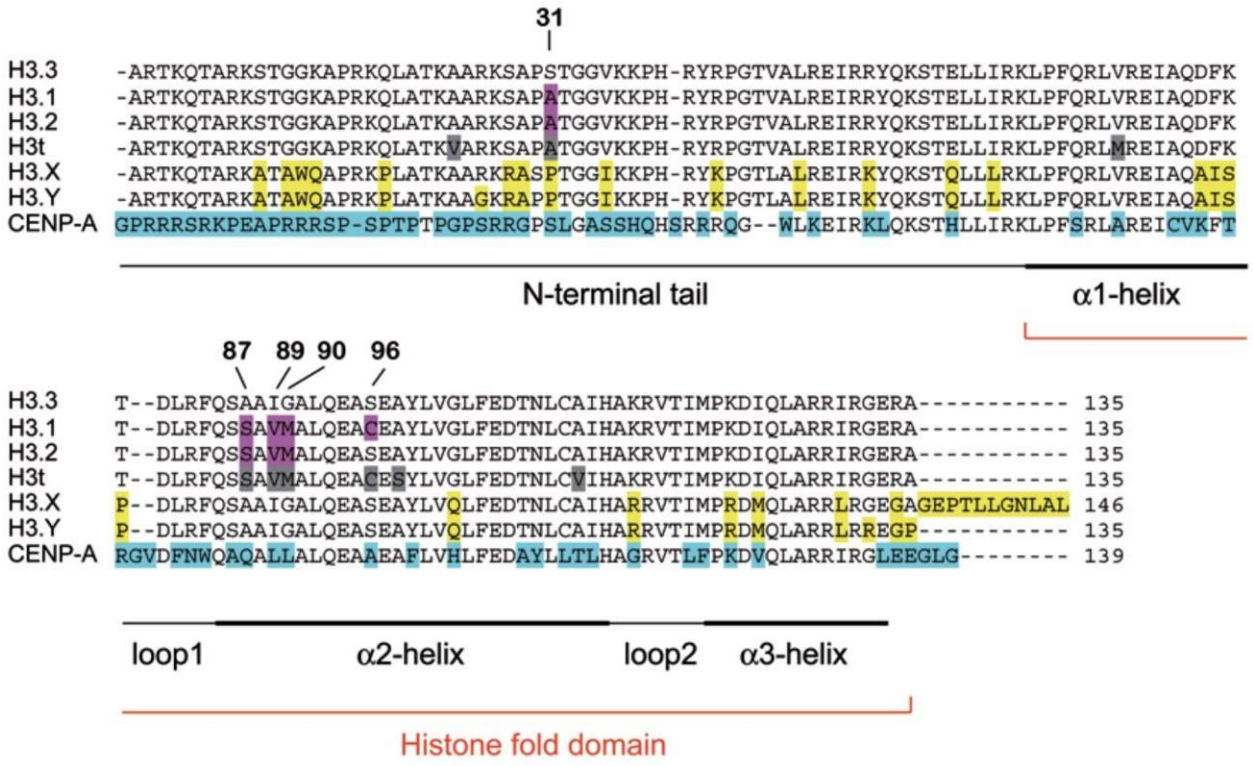

Figure 3. Sequence comparison of human H3 variants. The locations of the histone-fold motif's N-terminal tail and -helixes are shown. CENP-A is represented in blue color (adapted from Szenker et al., 2011).

2.4 Centromeric protein A (CENP-A) structure and regulation

CENP-A is made up of two different domains, a C-Terminal globular domain and an N-terminal domain which share the overall structure of canonical core histones. CENP-A globular domain is conserved across species and shares 62% of its sequence. The structure of the CENP-A nucleosome has been modeled as both an octosome and a hemisome. In the octasome model, two of each histone H2A, H2B, H4, and CENP-A forms a histone octamer. However, in the hemisome model, each of the histones H2A, H2B, H4, and CENP-A is represented by one (Figure 4a). CENP-A is one of the most studied H3 histone variant, which serves toward the steady transfer of a biological process during cell divisions. (Müller & Almouzni, 2017). In the cell cycle process, CENP-A inclusion is strictly controlled in the S phase. After the S phase, CENP-A is dispersed when the cell entered the G2 where it is produced again (Jansen et al., 2007).

Among these stages, the G1 phase, human cells begin to recruit CENP-A. CDK-dependent phosphorylation of M18BP1 regulates its recruitment (Silva et al. 2012) (Figure 4b). CENP-A plays an important role and serves as a marker and epigenetic descriptor of centromeres while contributing stabilization of the genome (Sitbon et al., 2017) Scientists prove that deficiency of CENP-A resulted in mitotic and nuclear defects which leads to senescence in different eukaryotic species (Bodor et al., 2014). During the cell cycle, CENP-A replaces canonical H3, with this replacement CENP-A functions as remodeling chromatin. Moreover, sustaining this process is critical for chromatin stability during cell cycle phases as well as the organism's long-term viability (Allshire & Karpen, 2008).

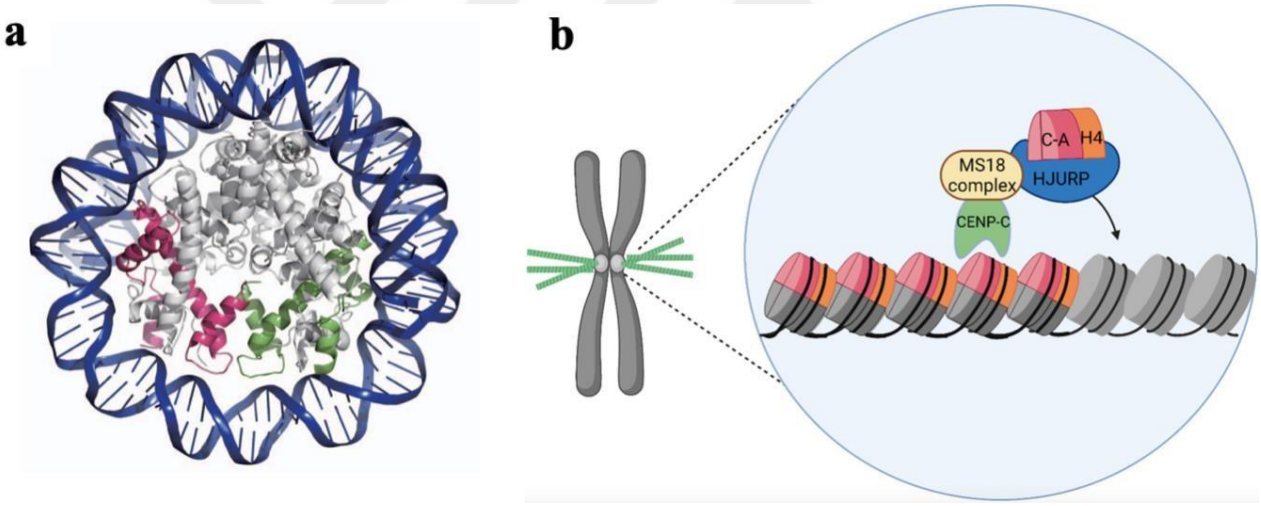

Figure 4. CENP-A structure and localization to centromeres. CENP-A nucleosome structure is shown (adapted from Tachiwana et al., 2011) (a) Before HJURP can bind to centromeres, the Mis18 complex attaches to CENP-C. Afterward, HJURP guides CENP-A to centromeric chromatin for placement in nucleosomes under the guidance of the protein (adapted from Morrison & Thakur, 2021). (b)

2.4.1 The Amino-Terminal of CENP-A

CENP-A N-terminal sequence is different from other H3 variants. There have been several studies to reveal the N-terminal functions of CENP-A. However, due to evolutionary perspective, and sequence differences in many species exact function of the N-terminal domain remains an open

question. In Jing et al. (2017) study they found two structural motifs of CENP-A N-terminal: $R^{42}R^{43}R^{44}$ and $K^{49}R^{52}K^{53}K^{56}$ play a role in CENP-A accumulation in the nucleus. Another study which used C. elegans as a model organism revealed that the N-terminal domain of CENP-A is required for proper centromeric chromatin assembly. They show that the N-terminal of CENP-A has gained part of the role of the specialized chaperone/targeting factor HJURP/Scm3 and has become required for loading into chromatin. (de Groot et al., 2021). Furthermore, there are studies focusing on PTMs in the N-terminal of CENP-A. For example, Sathyan et al. (2017) showed that N-terminal trimethylation of the CENP-A tail contributes to cell survival. In depletion of N-terminal trimethylation signal, CENP-T and CENP-I CCAN parts of the centromere cause loosen the chromosomes and resulted in spindle pole deformity. Important cellular events such as nuclear import, DNA interaction, and centromeric targeting in human cells all rely on arginine and lysine-rich motifs in CENP-N-tail.

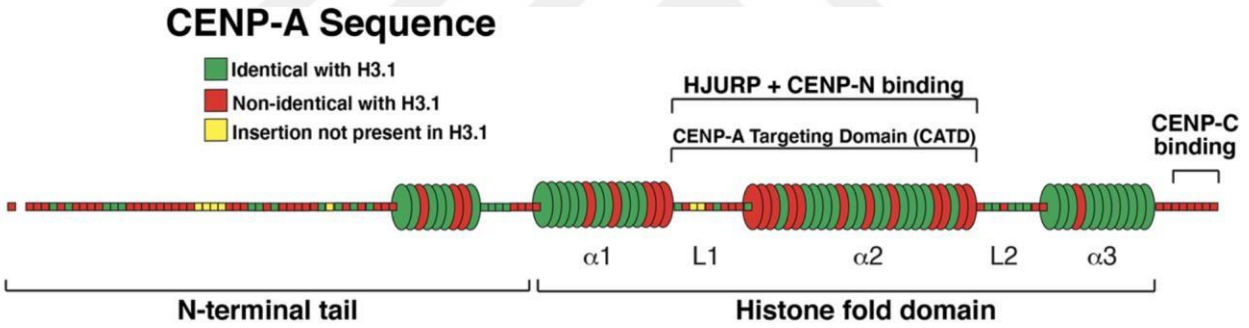

Figure 5. Representation of human CENP-A protein primary structure. The first loop and second alpha-helix in the histone fold domain are required for CENP-A centromere targeting. Consequently, this area is called the CENP-A targeting domain (CATD). Through the direct binding of the main kinetochore proteins, CATD, one of the functionally important structural units of CENP-A plays role in chaperone specificity and centromeric targeting. (Shuaib et al., 2010). CENP-N and CENP-C, CENP-A nucleosome sequences also provide centromere-specific activities. CENP-N connects to CENP-A by using the CATD domain of CENP-A. CENP-C interacts with the CENP-A nucleosome's C-terminal tail, histones, and CATD. The N-terminal of CENP-A has been linked to the recruitment of kinetochore proteins in many species (adapted from McKinley & Cheeseman, 2015).

2.4.2 Phosphorylation of Serine 7 Residue

There have been published contradictory data related to CENP-A S7p role. Since data are conflicting, the precise function of CENP-A S7p remains unclear. Aurora A initiates CENP-A S7p, which is sustained by Aurora B and C during telophases. According to a previous study, mutations at CENP-A Ser7 seem to affect the dynamics of Aurora B partitioning among chromosomes but have no effect on the localization of passenger proteins at midbodies in cytokinesis, chromosomal separation, or alignment. (Zeitlin et al., 2001) On the other hand, Kunitoku et al. (2003). discovered CENP-A S7A (serine to alanine conversion) expression delays prometaphase and misaligns chromosomes. Another study using mutational research postulated that CENP-A S7p controls CENP-C interaction to centromeres. Moreover, using CENP-A S7 mutants, they found that the CENP-A may be connected to CENP-C through phospho-binding 14-3-3 protein. As a result, the CENP-A S7A variant led to CENP-C loss, mitotic errors, and cell death. (Goutte-Gattat et al., 2013) Furthermore, it has been discovered that inhibiting CENP-A S7p resulted in sister chromatid cohesion problems, although there was no indication of defective kinetochore assembly. (Eot-Houllier et al., 2018). Serine 7 starts to get phosphorylated in prophase, and attains a peak in prometaphase, after that it begins to decline in anaphase. According to research by Barra et al. (2019), CENP-A is phosphorylated at serine 7 residue during the cell cycle and is not essential for centromere function. They target both alleles of CENP-A and the replacement process revealed that S7p does not play a role in CENP-C recruitments and chromosome segregation. However, they also investigate the role of serine 15, 16, 18, and 26 residues in the N-terminal domain of CENP-A by mutating them into arginine and alanine amino acids. Results suggested that serine 7 phosphorylation does not affect the functionality of CENP-A while S16 and S18 are essential for recruiting CENP-C and centromere function. Supporting this work, human serine 15 and serine 18 have previously been identified as important PTM sites for mitosis with respect to centromere integrity. (Bailey et al., 2013; Takada et al., 2017). As we know the sequence of S7p CENP-A is not conserved in other species. Also, the N-terminal tail of CENP-A from other mammals has not been shown to be phosphorylated. In this study, we aim to understand the S15/S16 phosphorylation site which is believed to function as a human CENP-A S7p (Table 1.)

Table 1.A summary of S7 phosphorylation-related research.

Findings	Strategy/Model Organism	Reference Study
• The completion of cytokinesis and the establishment of the location of Aurora B. • No significant change in the chromosomal order.	Using site-directed mutagenesis, S7 is changed to alanine (S7A). Performed in HeLa cells.	(Zeitlin et al., 2001)
• Aurora-A phosphorylation of CENP-A on S7 in prophase is important for kinetochore activity. • Delay in prometaphase and chromosomal misalignment.	Produced HeLa cell lines with GFP-fused wild-type CENP-A compared with mutated CENP-A-(S7A)	(Kunitoku et al., 2003)
• Blocking S7p causes mitotic defects and cell lethality. • Regulating CENP-C localization and binding through the centromere.	Created HeLa cell lines expressing a non-phosphorylatable GFP–CENP-A–S7A mutant resistant to siRNA.	(Goutte-Gattat et al., 2013)
• CENP-A S7p protects against premature centromere cohesion loss during chromosomal alignment.	HeLa cells that overexpress a GFP-CENP-A-S7A construct exhibit chromosomal misalignment.	(Eot-Houllier et al., 2018)
• CENP-A S7p is not essential for proper centromere dynamics and function.	CRISPR/Cas9 is used to change the endogenous CENP-A allele to an S7 non-phosphorylatable variant.	(Barra et al., 2019)

2.5 Genome engineering and CRISPR-Cas9

The goal of recombinant DNA technology is to edit an organism's genome from the outside in order to achieve advanced and desirable traits in live organisms. Its goal is to make the required mutation by combining DNA fragments from diverse sources with the desired gene sequence and injecting them into the suitable vector. Gene modification technology, which began with simple procedures, has enhanced the rate of gene targeting and modification, with starting usage of endonucleases (Khan et al., 2016) It is possible to introduce mutations at specific sites using the Cas9 endonuclease, a tool derived from the defensive mechanism of prokaryotes. The genome-editing method CRISPR-Cas9 (clustered regularly interspaced short palindromic repeats) is divided into two parts, the "guide" sgRNA (gRNA) and Ca9 nucleases. Cas9 endonuclease employs guide RNA to generate base pairs with DNA target sequences. Cas9 is a smart enzyme its biochemical features allow it to detect a single/double stranded DNA (Jiang and Doudna, 2017). Cas9 binding requires proto-spacer-adjacent motifs (PAM) which is 5'NGG'3 (N stands for A, G, C, T). After recognition double chain break is caused by the incision made in the desired area. (Figure 6). (Hille and Charpentier, 2016). The generated DNA damage can be repaired by two different methods with the DNA repair mechanism non-homologous end joining (NHEJ) or homology-directed repair (HDR) (Figure 7). The CRISPR-Cas9 technology is typically preferred over the ZFN and TALEN systems because of its simplicity, efficacy, and ability to target several genomic areas at once.

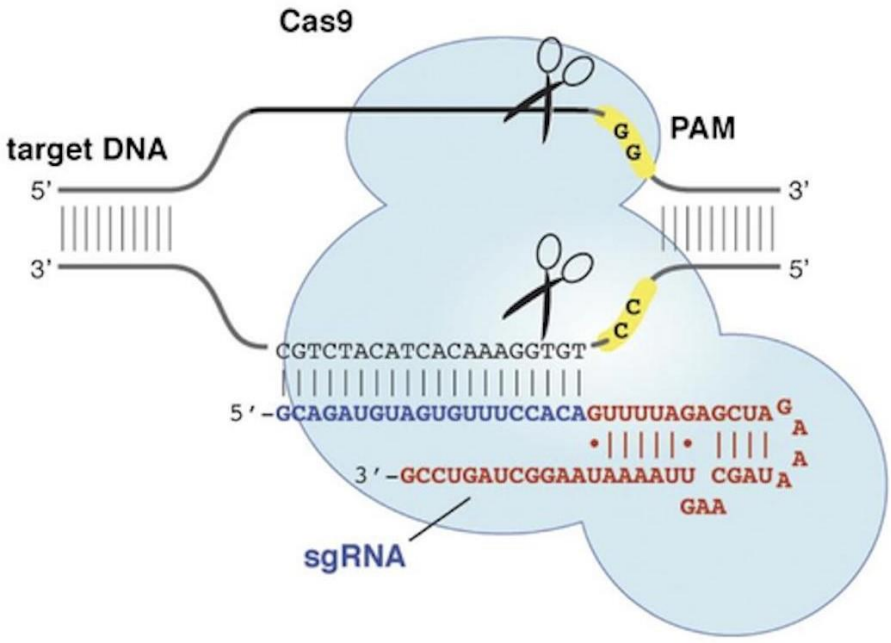

Figure 6. Representation of CRISPR-Cas9 working principle. Cas9 nuclease cleaves DNA in collaboration with sgRNA, which is complementary to the target sequence (adapted from Jinek et al., 2013).

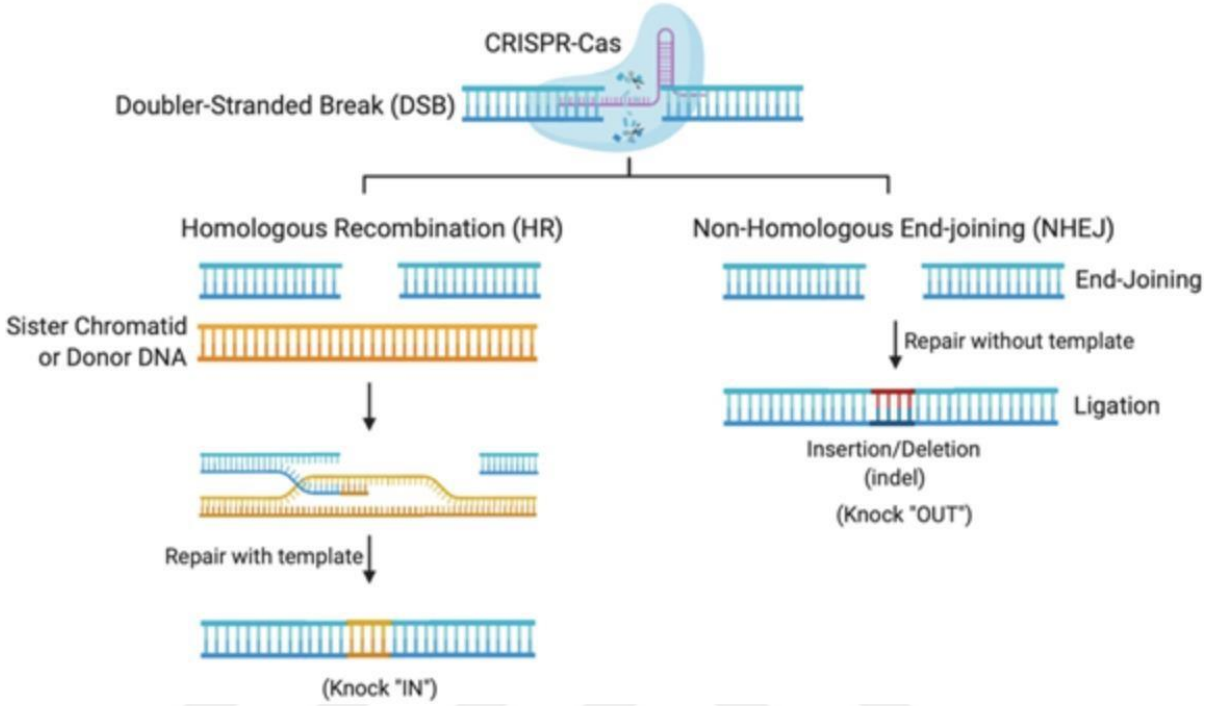

Figure 7. CRISPR-Cas repair systems. CRISPR-Cas requires DNA repair mechanisms to alter genes. The error-prone non-homologous end-joining (NHEJ) or homologous recombination (HR) are the most prevalent form of homology-directed repair (HDR). NHEJ generally results in unwanted repair sequences in the genome while HDR gives more precise editing with robust repair substrates such as sister chromatid and homolog repair donors (adapted from Shalaby et al., 2020).

2.5.1 Gene editing with the CRISPR-EZ system

The existing method of microinjecting CRISPR gene editing materials (plasmids, mRNA, sgRNAs) into pronuclear-stage embryos remains rate-limiting, despite the fact that CRISPR/Cas9 technology effectively edits genomes. As a result, the CRISPR-EZ system was developed by Modzelewski et al. (2018). This system is based on the electroporation of RNP into embryos **(**Figure 8.) Compering the other pronuclear and cytoplasmic microinjection methods CRISPR-EZ allows a simpler and facilitated way of editing.

CRISPR-EZ accomplishes 100% delivery of Cas9/single-guide RNA in C57BL/6J and C57BL/6N mouse strains, promoting indel mutations exon deletions, point mutations, and insertions.

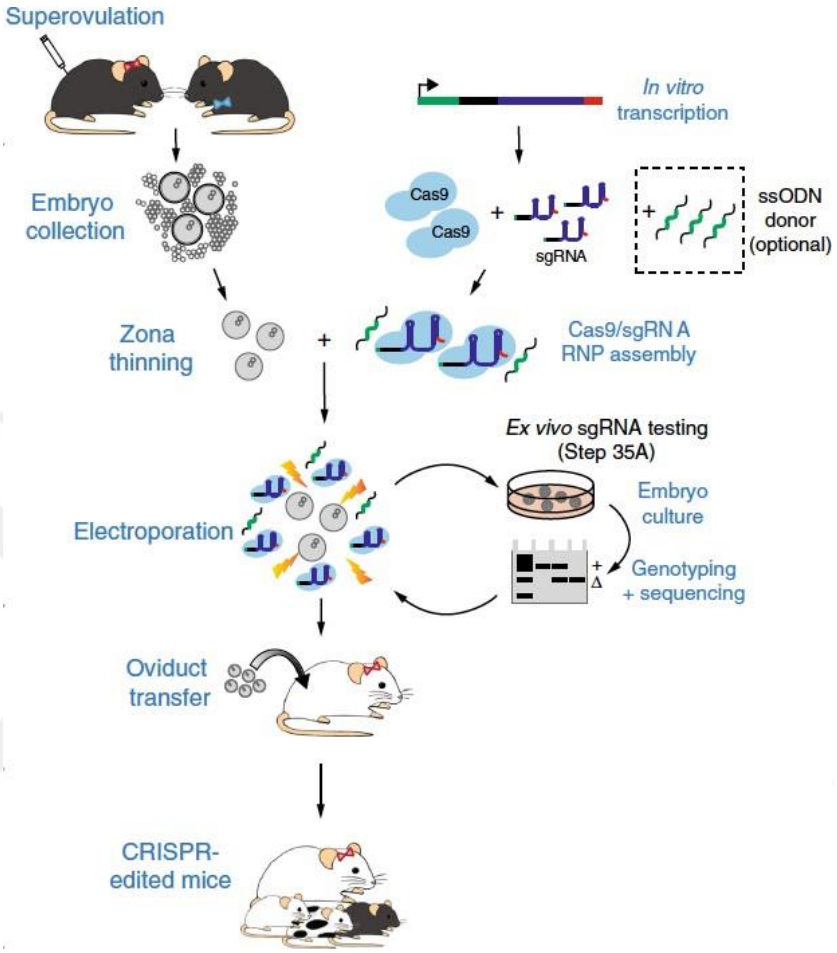

Figure 8. CRISPR-EZ pipeline. Researchers use PCR, in vitro transcription, RNA purification, and RNP assembly to generate functional Cas9/sgRNA complexes. Afterward, operate surgeries to obtain pronuclear-stage embryos from super-ovulated females for RNP electroporation. After cultivating pronuclear-stage embryos morula or blastocyst stage, genotyping and restriction analysis were applied for checking the editing rate (adapted from Modzelewski et al., 2018).

2.5.2 Asymmetric HDR strategy

Via using error-prone non-homologous end joining (NHEJ), Cas9 may easily make edited organisms while the effectiveness of exact sequence substitution by homology-directed repair (HDR) is significantly lower. In Richardson et al. (2016) study, they revealed that Cas9 separation from double-stranded DNA substrates is weak, while Cas9 asymmetrically releases the 3 ends of the cleaved DNA strand which is not complementary to the sgRNA before complete detachment. According to the study, the asymmetric part of the HDR allows for quick Cas9 dissociation after creating a nick at the double-strand compering to conventional HDR design. With this practice, genomic surveillance factors, and machinery of DNA damage substrates repair DSB at the desired site more efficiently. With a domino effect, quicker Cas9 dissociation results increase the progression of repair. In this study, they claimed that with an asymmetric HDR design, the rate of HDR editing could raise up to %60 in human cells (Figure 9). We employed standard HDR (ssODN) for Tyr editing, while an asymmetric HDR approach was used for CENP-A editing to aim for increased editing efficiency (Figure 10).

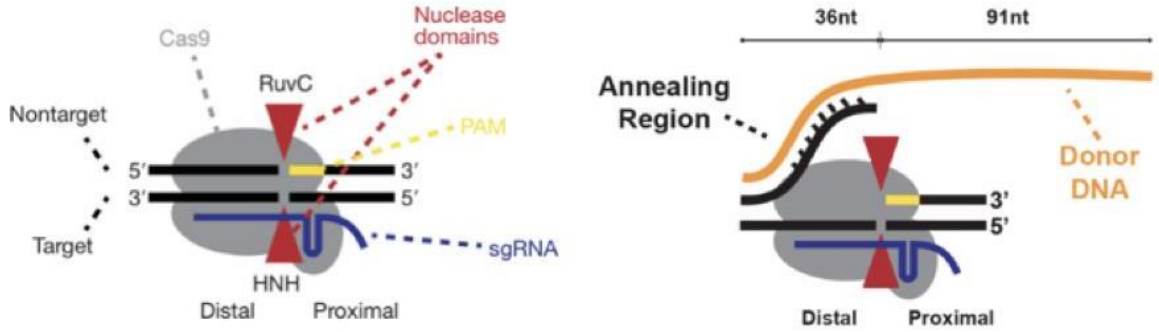

Figure 9. Demonstration of Cas9 and DNA interaction. Cas9 endonuclease (represented in grey color) binds DNA. At the non-target strand, PAM-Cas9 cooperation is shown and at the target strand, sgRNA-DNA annealing is demonstrated. The nuclease domains RuvC (His840) and HNH (Asp10) cleave both strands illustrated with red triangles (adapted from Richardson et al., 2016).

Figure 10. Asymmetric HDR design for CENP-A editing. Asymmetric HDR design used in CENP-A editing.

3. MATERIALS AND METHODS

3.1. Materials

Gotaq G2 Flexi DNA Polymerase (M7805) was purchased from Promega. Q5® High-Fidelity DNA Polymerase (M0491L), Deoxynucleotide (dNTP) Solution Mix (N0447L), EcoRI-HF® Restriction Enzyme (R3101S), PstI Restriction Enzyme (R0140S), HiScribe T7 High Yield RNA Synthesis Kit (E2040S), Monarch RNA Cleanup Kit (T2040L) and Proteinase K (P8107S) supplied from NEB. HinfI Restriction Enzyme (ER0801), GeneRuler 100bp Plus DNA Ladder (SM0322), GeneRuler 50 bp DNA Ladder (SM0373), GeneJetPCR Purification Kit (K0702), Opti-MEM reduced serum media (11058021), Fast Digest Buffer (B64), HinfI Restriction Enzyme (FD0614), TBE-Urea Gel 10%,-10well (EC6875) were purchased from Thermo Scientific. Greiner Bio-One supplied the Microcentrifuge Tubes (616201). 10ul filtered sterile tips (10500064) from Gibco. Alt-R® S.p. Cas9 Nuclease V3 (1081059) and Cas9 electroporation enhancer (1075915) were bought from Integrated DNA Technologies. Microcentrifuge tubes, polypropylene (616201) from Greiner Bio-One, PCR tubes (123.01.002) from Isolab, Methanol (34860-2.5L-R), isopropanol (34863-2.5L), and ethanol (32221-2.5L) SafeView Classic (G108) were purchased from ABM. All reagents were of analytical grade.

Primers used in this study are given in Table 2.

Table 2. The list of primers used in this study.

Sequence	Purpose
GGATCCTAATACGACTCACTATAG	IVT FWD generates the IVT template by PCR, universal
AAAAAAGCACCGACTCGG	IVT REV generates the IVT template by PCR, universal
TCTTTTCGGAGACACTCAAATCA	sgTyr F1 for screening
TCTGTACAATTTGGGCCCCC	sgTyr F2 for screening
GCTTTCAGGCAGAGGTTCCT	sgTyr R1 for screening
CACCGAAGGAGGAGACCCTCCAGCC	mouse CENPA sgRNA1 Forward
AAACGGCTGGAGGGTCTCCTCCTTC	mouse CENPA sgRNA1 Reverse
CACCGGTCCAGGCGCCGGGCTGGA	mouse CENPA sgRNA2 Forward
AAACTCCAGCCCGGCGCCTGGACC	mouse CENPA sgRNA2 Reverse
TTTTTGAACTGCTGGCGACC	mouse CENPA screening primer F1
CATTACCCCTACGCGAGGTT	mouse CENPA screening primer R1
CTTGCTCGCGTTCGGTTTC	mouse CENPA screening primer F2
CCCTGCTGTAAACCGGTCAG	mouse CENPA screening primer R2

3.2 Method

3.2.1 sgRNA synthesis

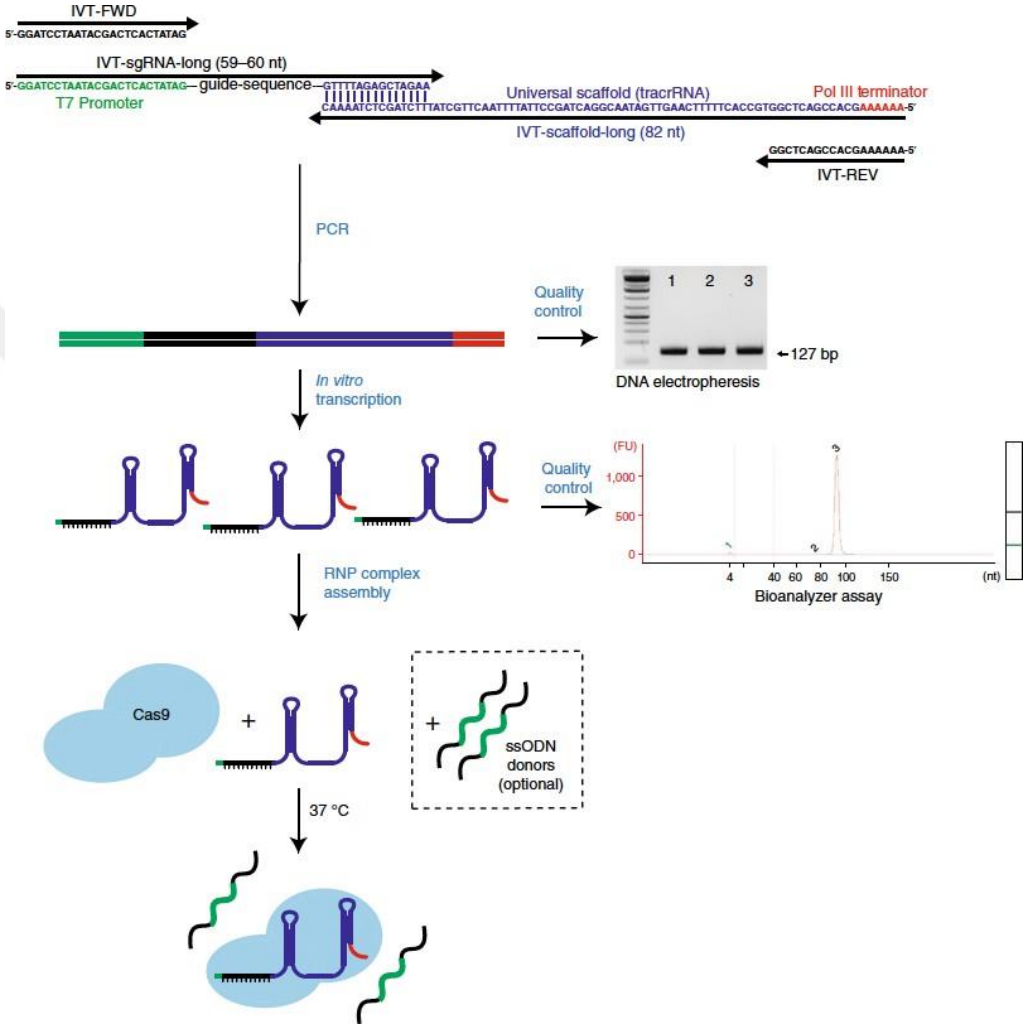

Figure 11.Schematic demonstration of sgRNA synthesis with in vitro transcription. A couple of PCR primers black correspond to IVT-Forward and IVT-Reverse. The common reverse template oligo shown in blue/red: IVT-scaffold-long and an oligo with a 5′ T7 promoter and sgRNA sequence represented in the color (green/black/blue: IVT-sgRNA-long) are among the components. A PCR reaction is required to create the DNA template for sgRNA production. This reaction produces a single 127-bp amplicon, which should be verified using gel electrophoresis. T7 in vitro transcription (IVT) is then used to produce sgRNAs. Before continuing to trials, the quality and amount of newly generated sgRNA were tested by using a Bioanalyzer or Urea gel (adapted from Modzelewski et al., 2018).

To create the DNA template for sgRNA in vitro transcription using PCR, the appropriate reaction mixture is prepared in a sterile RNase-free eight-well PCR strip tube.

Table 3. PCR set-up for sgRNA template synthesis.

Component	Amount (µl)	Final Concentration
H_2O	35.5	-
5x Q5 Reaction Buffer	10	1x
10 mM dNTPs	1	0.2 mM
IVT-universal-Forward (1uM)	1	0.02 µM
IVT-universal-Reverse (1uM)	1	0.02 µM
IVT-sgRNA oligo Tyr (100uM)	0.5	1 µM
IVT-sgRNA-Scaffold-long (100um)	0.5	1 µM
Q5 enzyme (2 U/µl)	0.5	0.02
Total	50	-

Table 4. PCR cycling conditions for sgRNA template synthesis.

Cycle Number	Denature	Anneal	Extend
1	95 C^0, 2 min		
2-31	95 C^0, 10 s	57 C^0, 10 s	72 C^0, 10s
32			72 C^0, 2min

- At this step, control the PCR amplicon with %2 agarose gel. The product should be at 127bp size (Figure 11).
- PCR clean-up produce is applied according to GeneJet-PCR purification Kit protocol.
- Prepare the following reaction mixture in an RNase-free eight-well PCR strip tube by gently pipetting the chemicals together.
- The NEB HiScribe T7 High Yield RNA Synthesis Kit includes all materials except the DNA template.

Table 5. Set-up for T7 in vitro transcription (IVT).

Component	Amount (µl)	Final Concentration
10x HiScribe Reaction buffer	2	1x
ATP (100 mM)	2	10mM
GTP (100 mM)	2	10mm
CTP (100 mM)	2	10mm
UTP (100 mM)	2	10mm
DNA template (Step 3)	8	25ng/µl
T7 RNA polymerase mix	2	-
Total	20	-

- IVT reaction mix is incubated for over 18h at 37C^{o} in a thermocycler machine.
- After incubation, 1µl RNase-free DNase I ((2 U/reaction) is added to PCR tubes and incubated for 20 mins.
- For the clean-up process, the Monarch RNA-Clean-up kit is used and followed the instructions of the kit.

3.2.2 sgRNA purification by Monarch RNA-Cleanup Kit

1.) 100 µl RNA Clean-up Binding Buffer is added to the 50µl sample. (If the sample is not 50µl, arrange up to 50 µl using RNase Free-water.)

2.) 150 µl of ethanol (>95%) was added to the sample. Mixing is done by flicking the tube, not the vortexing.

3.) The reaction is transferred into collection tubes found on the kit. After loading the sample, centrifuged at 16,000xg for around 1min.

4.) The column is reinserted into the collection tube after centrifugation and a 500µl clean-up buffer is added. Discard the liquid substance.

5.) The wash step is repeated. (Step 4)

6.) The column is placed into the sterilized 1.5ml microfuge tube.

7.) sgRNA is eluted by using 20µl RNase-free ddH_2O according to the length of the sgRNA.

3.2.3 Superovulation and Mating

CRISPR-EZ method requires pronuclear stage embryos isolated from young (four weeks old) C57BL6 female mice. Because one female mouse can produce roughly 20 embryos, and several embryos may be lost during the manipulation phases, this study required ten female mice for superovulation and embryo collection. On Day 1, mice received an intraperitoneal injection of 5 IU PMSG. On Day 3, 5 IU of hCG was injected to stimulate ovulation. Following an hCG injection, each female was paired with one fertile stud male mouse (C57BL6). CD1 female mice to be used as hosts for embryo transfer were paired with vasectomized male mice on the day that C57BL6 mice were mated in order to produce synchronized pseudo pregnant mice.

3.2.4 Embryo Isolation and Manipulation

Females were taken one day after mating which corresponds to Day 4, for a copulation plug check. The cervical dislocation was used to euthanize females with plugs. Steps for oviduct collection and dish prepping were carried out according to Modzelewski et al. (2018c). The female mouse's oviducts were isolated and placed in the oviduct dish, which was maintained at 37°C with the help of a heater. One oviduct was placed in the dish after ten female mice's oviducts were collected. The oviduct's ampulla was found using a stereomicroscope, and a forceps was used to cut the ampulla. After cumulus cells were detached, pronuclear stage embryos were harvested with mouth pipetting using a pulled glass capillary. To wash off extra cumulus cells, collected embryos were placed in a wash dish which is including 1ml GLOBAL HEPES Media with BSA. A drop of 50L GLOBAL Media with BSA was placed into a dish for culturing. In total, 12 drops were placed in a single dish. Mineral oil was poured into the dish until all of the drips were coated, and the dish was then equilibrated in a 5 percent CO2 incubator at 37 ℃ and %95 humidity. After electroporation, the embryos were taken and placed in these drops. 10 embryos were delivered for each drop. Embryos were cultivated in the incubator for 4 days in an embryo culture plate. When embryos reach the morula or blastula stages, they were gathered into clean PCR tubes which include 10ul HotShot buffer. Samples (embryo mix) heated for 2 minutes in HotShot Lysis Buffer at 95°C. 10μL HotShot Neutralization Buffer was added to each PCR tube (applied according to

Truett et al., 2000). The mixture was kept at -20°C as a DNA template for further genotyping procedures.

3.2.5 Ribonucleoprotein complex (RNP) Mix preparation

Firstly, sgRNA and Cas9 are mixed with opti-MEM on the clean PCR tube. 2ul HDR is added and incubated for 10 min at room temperature before electroporation. The mixture (RNP mix) was placed in a 0.1-cm-gap electroporation cuvette. Embryos were subsequently electroporated with a square-wave technique in a Bio-Rad Gene Pulser XCell device using the conditions listed in (Table 6). Electroporated embryos were gathered on a dish after being washed three times with 50L Opti-MEM. The embryos obtained as demonstrated in section 3.3.1 were added to the RNP solution by mouth pipetting.

Table 6. Electroporation conditions.

Condition	Value
Voltage	30V
Pulses	4-6
Pulse length	3ms
Pulse interval	100ms

Table 7.RNP-Mix set-up for Tyr editing.

Ingredients	Amount
Tyr-sgRNA (3.2ug/ul)	0.8µl
Tyr-HDR oligo (100uM)	2 µl
Cas9 IDT (61uM)	1.3µl
Opti-MEM	15.9µl
Total	20µl

Table 8. RNP-Mix set-up for CENP-A editing.

Ingredients	Amount
CENPA-sgRNA (3ug/µl)	0.8µl
CENP-A HDR oligo (100µM)	2µl
Cas9 IDT (61µM)	1.3µl
Opti-MEM	15.9µl
Total	20µl

3.2.6 Genotyping PCR of Tyr-edited embryos

CRISPR-EZ settings were optimized for editing efficiency and embryo viability.

The NHEJ and HDR editing techniques for exon 1 of the Tyr gene are presented. NHEJ editing successfully anneals a HinfI site disrupting Tyr gene function (Figure 12). PCR conditions and set-up are demonstrated in (Tables 9 and 10).

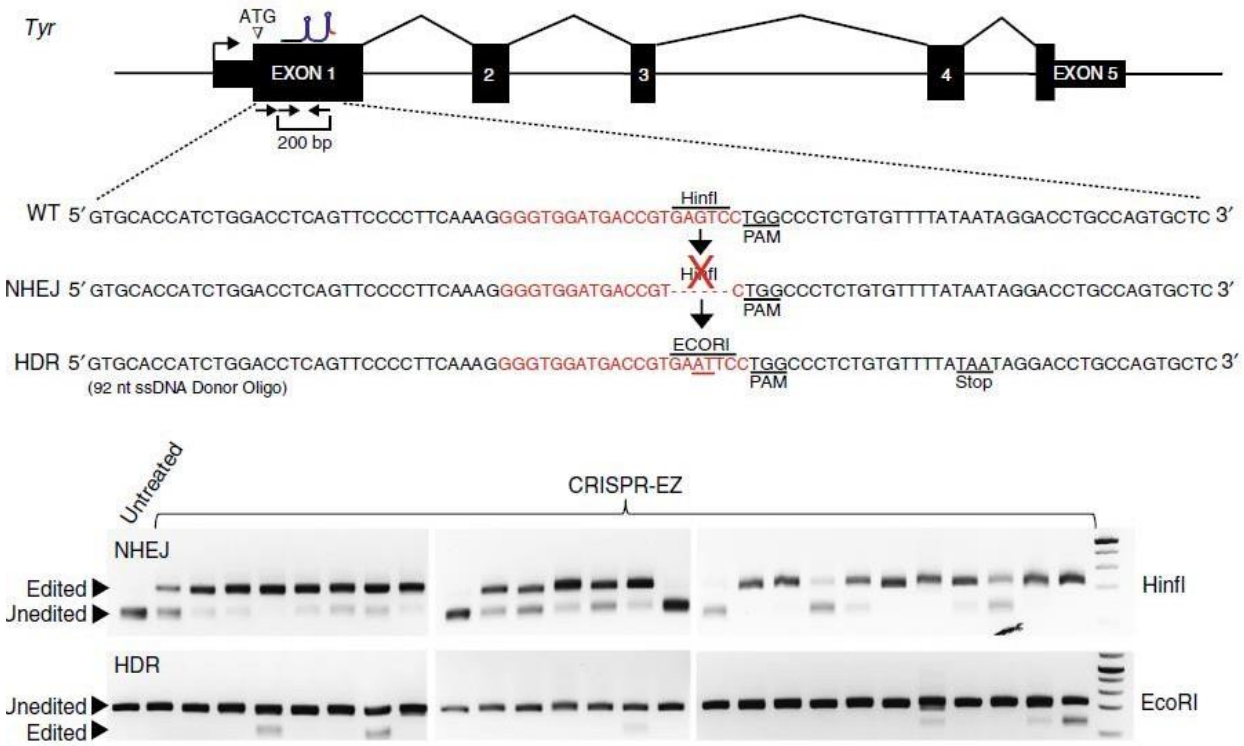

Figure 12. Schematic representation of genotyping strategy for Tyr-editing. The HinfI site is replaced with an EcoRI site in a successful HDR editing, resulting in a frameshift mutation that disables Tyr gene function (adapted from Modzelewski et al., 2018)

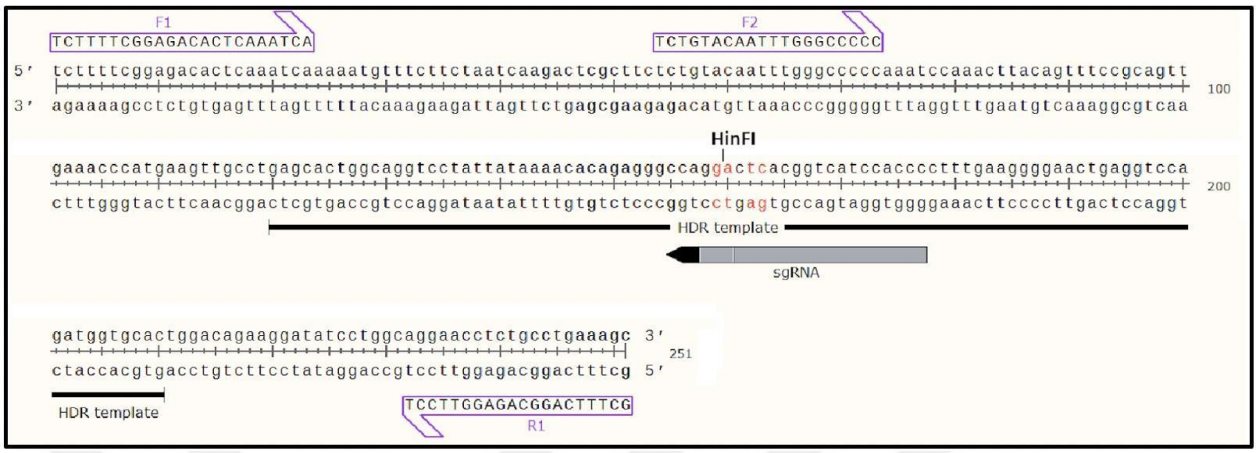

Figure 13. The arrangement of screening primers for Tyr-gene locus. After Nested PCR, amplicons should give 200bp and amplicons were analyzed by using HinfI and EcoRI enzymes. EcoRI digestion shows NHEJ edited embryos while HinfI restriction indicates WT phenotype.

Table 9. Nested PCR set-up used for genotyping Tyr-edited embryos.

Component	Amount	Final Concentration
5x GoTaq Green buffer	2µl	1x
dNPTs	0.2µl	-
$MgCl_2$	0.6µl	-
sgTyr F1 for screening	1µl	1mM
sgTyr R1 for screening	1µl	1mM
GoTaq enzyme	0.1µl	-
H_2O	2.1µl	-
DNA	3µl	-
Total	10µl	-

Table 10. Thermocycler conditions of Tyr-Genotyping.

Cycle Number	Denature	Anneal	Extend
1	95 C^0, 2 min		
2-31	95 C^0, 10 s	60 C^0, 10 s	72 C^0, 10s
32			72 C^0, 2min

After applying the first PCR shown in Table7, 1/100 diluted first PCR product is used for the second PCR template. Thermocycler conditions are the same as indicated in (Table 10). The expected amplicon should be 200bp size.

Table 11. PCR conditions of Tyr-Genotyping.

Component	Amount	Final Concentration
5x GoTaq Green buffer	4µl	1x
dNPTs	0.4µl	-
$MgCl_2$	1.2µl	-
sgTyr F2 for screening	1µl	1mM
sgTyr R1 for screening	1µl	1mM
GoTaq enzyme	0.1µl	-
H_2O	2.1µl	-
DNA	11.3µl	-
Total	20µl	-

3.2.7 Restriction Analysis for Tyr-Editing

Successful HDR editing creates EcoRI one site at the Tyr locus, as indicated in section 3.4, whereas HinfI restriction is employed to detect non-edited embryos as a negative control.

Table 12. Restriction analysis ingredients for Tyr-editing.

Component	Component	Amount (1x reaction)
HinfI enzyme (1U)	EcoRI enzyme (1U)	1µl
DNA (second PCR)	DNA (second PCR)	5µl
Cutsmart Buffer	Cutsmart Buffer	1µl
ddH_20	ddH_20	3µl

3.2.8 Genotyping strategy for CENP-A

For the genotyping of CENP-A again Nested PCR amplification is used. which allows clear bands for further restriction analysis. HDR introduces a novel PstI restriction site.

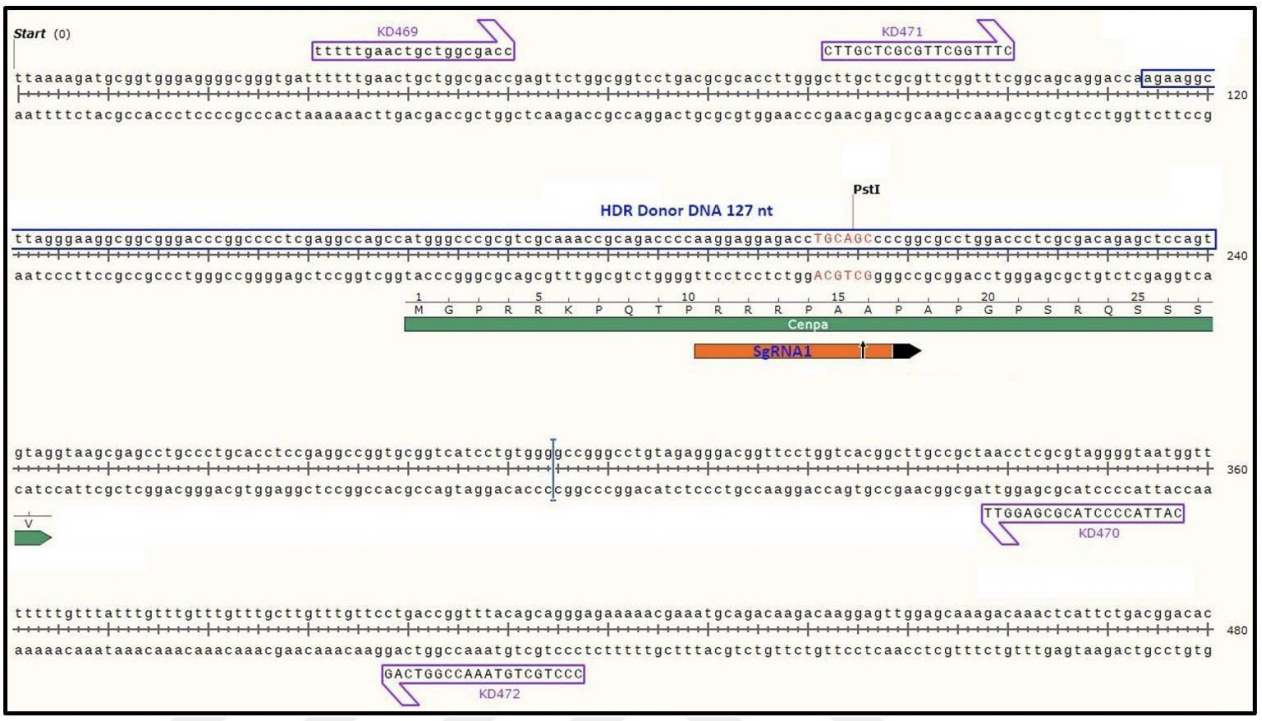

Figure 14. Genotyping and screening strategy for CENP-A.

3.2.9 DNA extraction protocol for CENP-A mouse tissues

- Nail or tail from the mouse taken.
- 10µl of 20mg/ml Proteinase K is added directly into the samples.
- Water bath or heat block adjusted at 55C°, and samples incubated overnight.
- Samples were taken from bath vortexed 5 min.
- 6M NaCl is prepared using double distilled water. 250µl NaCl(6M) is added to each sample.
- After 5 min vortexing, samples were centrifuged at 4C° 13.000rpm for about 10min.
- 500 µl isopropanol is added to each sample.
- Again, samples were centrifuged at 4C° 13.000rpm for about 10min.
- The liquid part should be removed carefully DNA is found at the bottom in pellet shape.
- For the washing step, 750 µl ethanol (%70) is added into microfuge tubes.
- Samples were centrifuged at 4C° 13.000rpm for about 10min.
- Removed the ethanol from the pellet and wait until it's dry.
- 30µl nuclease-free water is added and left at 4C° overnight.

First PCR ingredients and the amount is shown in the table.

Table 13. First PCR set-up for CENP-A.

Component	Amount	Final Concentration
5x GoTaq Green buffer	4µl	1x
dNPTs	0.4µl	-
$MgCl_2$	1.2µl	-
CENP-A F1 for screening	0.5µl	1mM
CENP-A R1 for screening	0.5µl	1mM
GoTaq enzyme	0.1µl	-
H_2O	10.3µl	-
DNA	2µl (from hotshot)	-
Total	20µl	-

For the template of the second PCR, 1/100 diluted first PCR product is used. At the result of the second PCR, the amplicon should be sized at 336p.

Table 14. Second PCR set-up for CENP-A.

Component	Amount	Final Concentration
5x GoTaq Green buffer	4µl	1x
dNPTs	0.4µl	-
$MgCl_2$	1.2µl	-
CENP-A F2 for screening	0.5µl	1mM
CENP-A R1 for screening	0.5µl	1mM
GoTaq enzyme	0.1µl	-
H_2O	11.3µl	-
DNA	1µl (1/100diluted)	-
Total	20µl	-

Table 15. Thermocycler conditions of CENPA-Genotyping.

Cycle Number	Denature	Anneal	Extend
1	95 C^0, 2 min		
2-34	95 C^0, 15s	65C^0, 10 s	72 C^0, 25s
35			72 C^0, min

3.2.10 Restriction Analysis for CENP-A-Editing

PstI digestion shows successful HDR-editing. The second PCR which gives 336bp should give two distinctive bands size at 213bp and 123bp after restriction analysis that indicates homozygous mouse. If there is a blurred band at the size of 336 in addition to 213-123bp bands this shows a heterozygous genotype.

Table 16. Restriction analysis ingredients for CENP-A.

Component	Amount (1x reaction)
PstI enzyme (1U)	1µl
DNA (second PCR)	5µl
CutSmart Buffer	1µl
ddH_20	3µl
Total	10µl

3.3 Workflow

This project is based on creating a mouse model for CENP-A N-terminal epigenetics investigations. The CRISPR-EZ method was chosen for the editing system. For getting the mouse model all steps demonstrated in (Figure 15) are applied after optimizations.

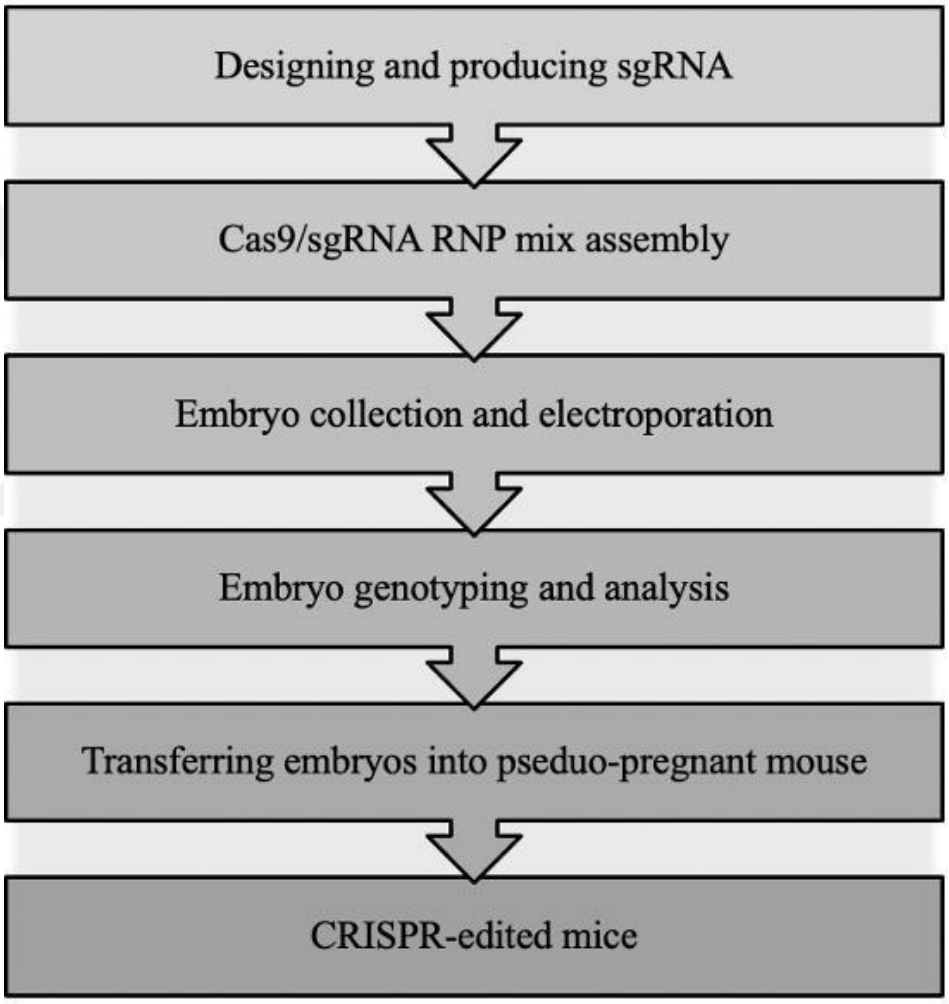

Figure 15. Workflow of the project.

4. RESULTS

4.1 Creating Tyr Mouse model

4.1.1 sgRNA synthesis and quality confirmation

sgRNA's produced by in vitro transcription method are analyzed by TBE-Urea gel. The left side of the figure shows the Tyr and CENP-A sgRNAs template which should be given exactly a 127bp amplicon. On the right side of the figure, for controlling the size of Tyr and CENPA sgRNAs, a previously produced and characterized sgRNA is used as a marker. Urea gel can remove secondary structure forms of RNA. In this figure, the intact band image confirms Tyr and CENPA sgRNAs are produced successfully (Figure 16).

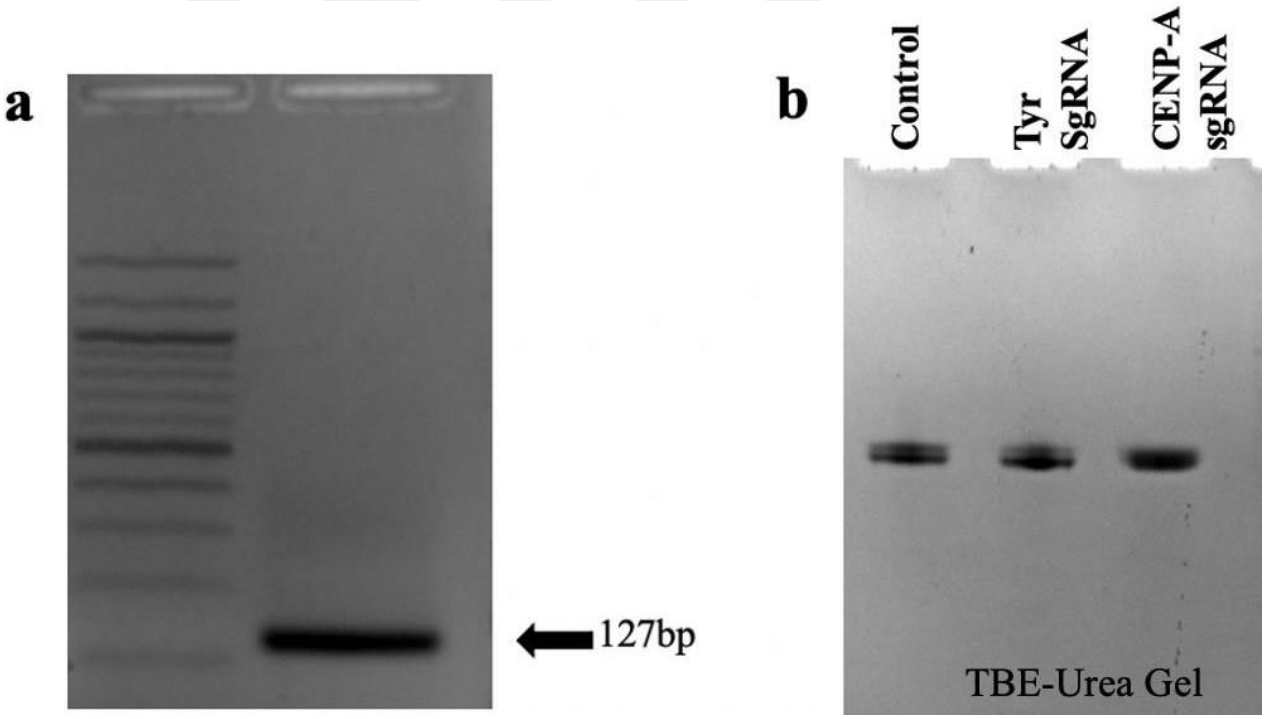

Figure 16. Quality confirmation of produced sgRNAs. Template synthesis control (a), sgRNA quality checking with %10x TBE urea gel, 200ng sgRNA is loaded into the gel. (b) After optimizing the condition of the urea gel, 100ng is decided to use for subsequent experiments.

4.1.2 Embryo genotyping

Embryos electroporated with Tyr-RNP mix genotyped using nested PCR method. After applying the Hotshot DNA extraction protocol Tyr locus amplified with KD-431(F) and KD-433(R). For getting a clear and bold band 1/100 diluted first PCR samples were used for applied second PCR with KD-432(F) and KD-433(R). Correct amplification of Tyr locus size should give 200bp as the figure indicates. In this figure, I analyzed 45 embryos 18 of them are at the stage at blastocyst while 27 are at the morula (Figure 17).

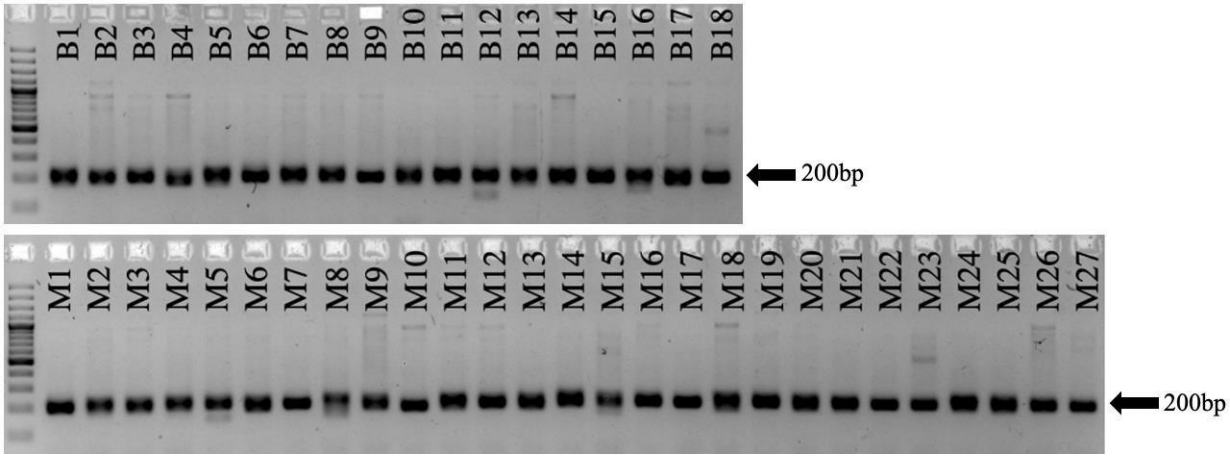

Figure 17. Nested PCR results of Tyr-RNP electroporated embryos. The extracted DNAs of 18 blastocysts and 27 morula stage embryos are amplified using the Nested PCR procedure, which should give 200bp size bands.

4.1.3 Restriction Analysis of Genotyped Tyr-Edited Embryos

For confirming NHEJ editing, two restriction enzymes are used to check the Tyr locus at exon 1. A successful NHEF editing disrupts the HinfI restriction site to EcoRI. With this strategy, we can conclude that DNAs that are cut by the HinfI restriction enzyme stand for non-edited Tyr locus while the EcoRI digest corresponds to successful HDR-editing. EcoRI and HinfI enzymes were used to digest chosen embryos in this figure. M14, M15, M16, and B6 have been HDR edited at the bottom (Figure 18b).

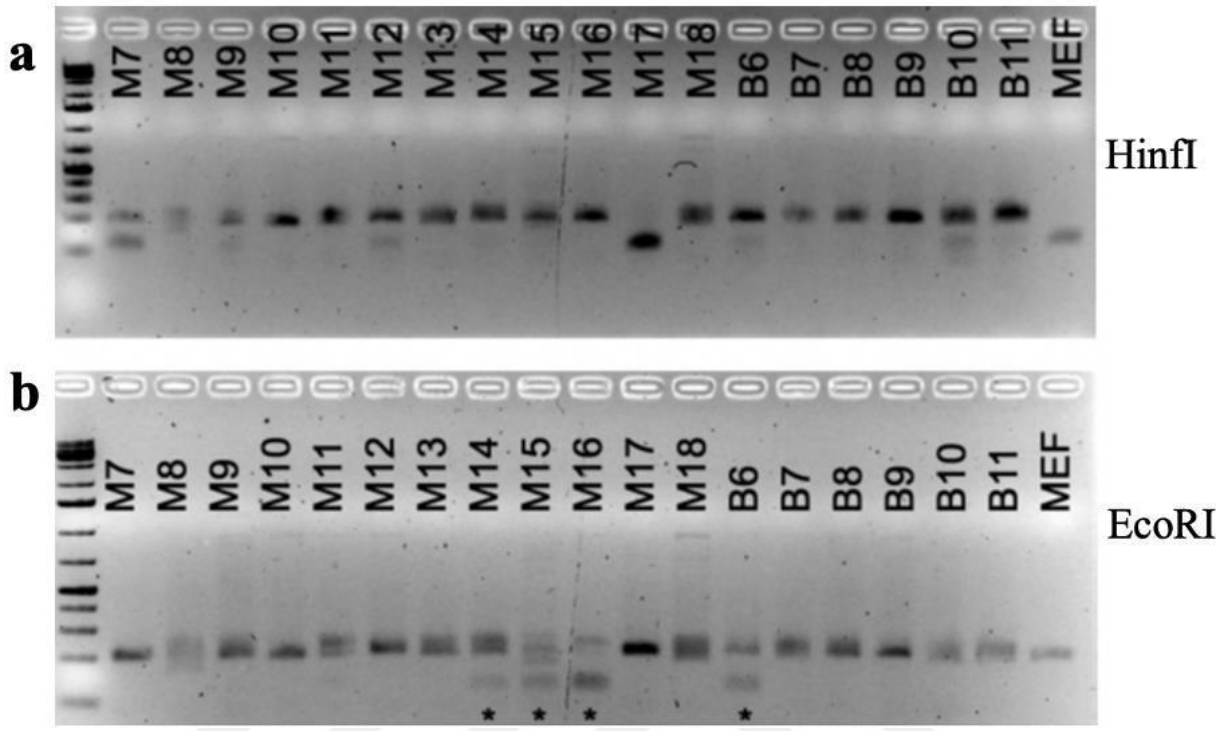

Figure 18. HinfI and EcoRI Restriction analysis of Tyr-RNP electroporated embryos. The majority of embryos had DSB at the Tyr locus, and HinfI sites were lost due to NHEJ or HDR repair. From the total PCR amplified embryo samples in Figure 17, only selected embryos were analyzed by restriction digestion. Asterisk shows the embryos with the EcoRI site, suggesting the presence of the HDR-mediated knockin allele.

4.1.4 Creating Tyr gene-edited mouse model

By using the CRISPR-EZ method, the brown pigment synthesis gene Tyrosinase was edited in the in vivo model. After getting a high editing ratio from the embryos experiment, at the next trial embryos were transferred into pseudo-pregnant mice to get an Tyr edited mouse model. We have obtained albino mice both with indel mutations and targeted knockin mutation at Tyr locus (Figure 19). After establishing the CRISPR-EZ system on Tyr locus, we proceeded with creating a mouse model for CENP-A N-terminal mutations.

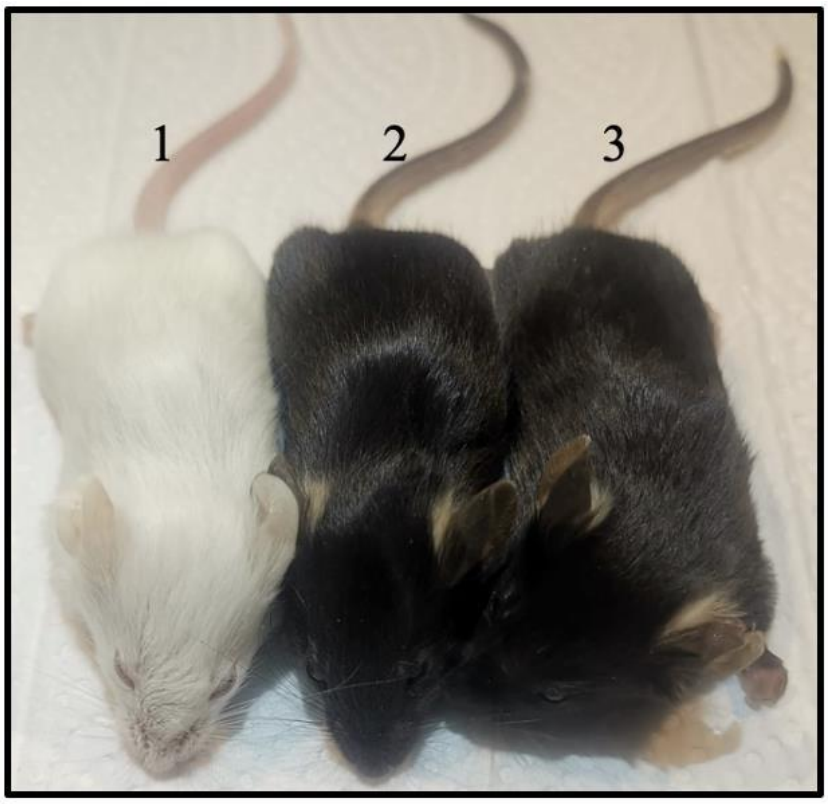

Figure 19. Representation of the Tyr CRISPR edited mouse model. Targeted modification of the Tyr gene results in albino coat color, whereas the other littermates display the WT black coat color phenotype of the C57BL/6 inbred strain.

4.2 Creating CENP-A mouse model

After optimizing the CRISPR-EZ protocols and creating a Tyr-edited mouse model, we applied the same strategy for the CENP-A knockin model. We aimed converting serine 15 and 16 into alanine. For increasing HDR efficiency, we used an asymmetric HDR design.

4.2.1 CENP-A mouse genotyping

CENP-A RNP electroporated embryos were transferred into pseudo-pregnant mice. Nested PCR is used for genotyping CENP-A edited mice. For the first PCR KD-469(F) and KD-472(R) are used. 1/100 diluted first PCR reaction mix is used for the second PCR template which is amplified with KD-471(F) and KD-472(R). Second PCR should give 336bp exactly in the figure

demonstrated. Bands seen above and below the 336bp size indicate indel mutations such as C4-C5 (Figure 20).

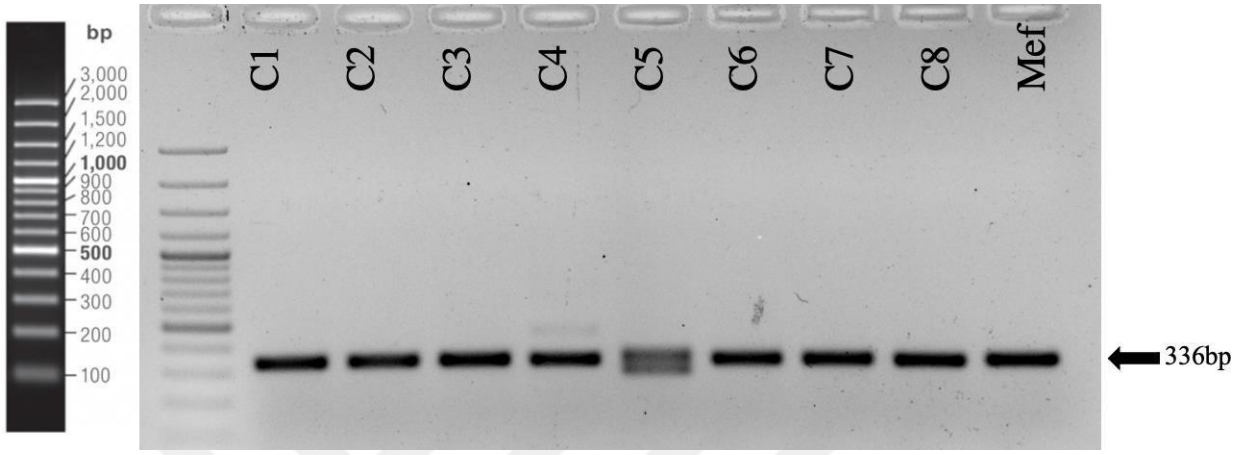

Figure 20. Genotyping of live-born pups after CENP-A CRISPR-EZ protocol (C1-C8). **C**ENP-A edited embryos were transferred into host CD1 mice. Lıve-born pups were genotyped by nested PCR. For the control (unedited WT), mouse embryonic fibroblast (MEF) genomic DNA was used. PCR products were separated by 2% agarose gel 90V around 1h.

4.2.2 Restriction analysis results of CENP-A edited mice

After CENP-A CRISPR editing, HDR introduces a novel PstI site at the mutation zone. A homozygous digestion pattern should give two bands at the size of 213bp and 123bp. The C1 mouse in the figure has a strong probability of being homozygous, whereas the C2, C3, C6, and C7 digestion patterns show the presence of the knockin mutation. These mice are potentially mosaic genetically and could as well carry additional indel mutations.

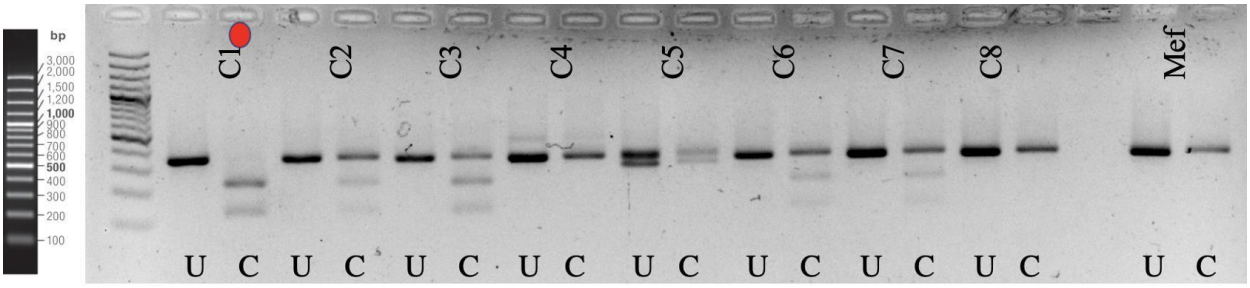

Figure 21. Restriction Analysis of CENP-A electroporated mice with PstI (C1-C8). Digested products run for 1.5 h at %2 agarose gel with 90V. MEF is used as the negative control (non-digested). A complete digestion reaction of 10ul is loaded which includes a 5ul PCR product digested with PstI.

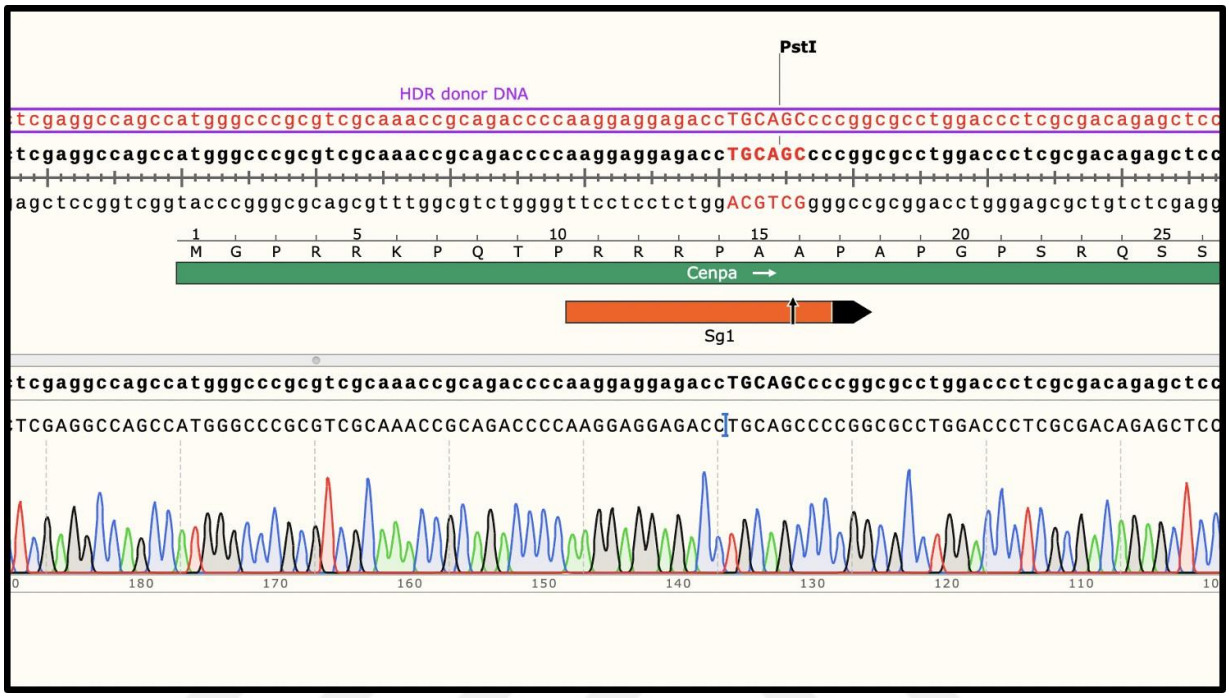

Figure 22. Sanger sequencing confirmation of C1 mouse. The figure shows that targeted serine 15 and serine 16 are converted to alanine successfully. TGCAGC sequence corresponds to the C1 mouse CENP-A N-terminal locus. PstI site is added via codon choice and silent mutations. Densitogram does not suggest the presence of additional alleles, although the presence of very large deletions that could not be amplified by our nested PCR protocol cannot be ruled out.

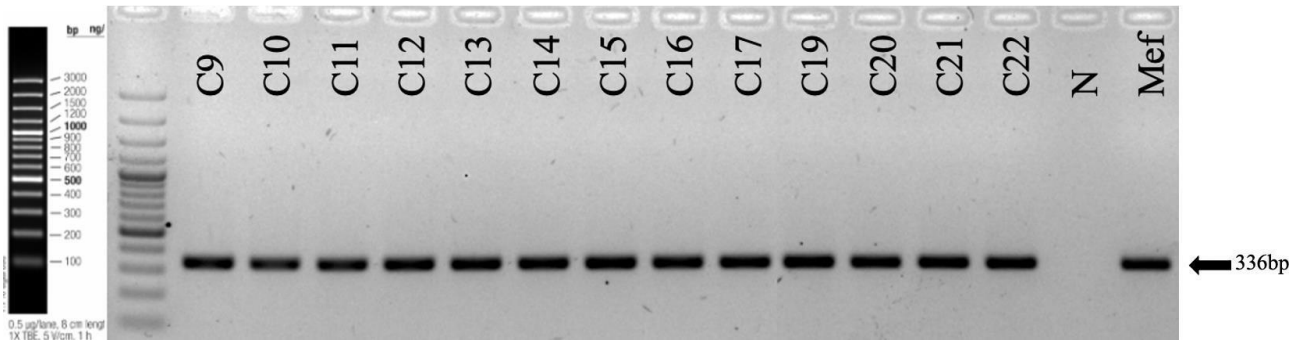

Figure 23. Genotyping of the live-born second-generation CENP-A edited pups (C9-C22). As shown in the diagram, genotyping pups gives a 336bp PCR product at the correct size. All amplicon lines are at the same size indicating that there are no indel mutations.

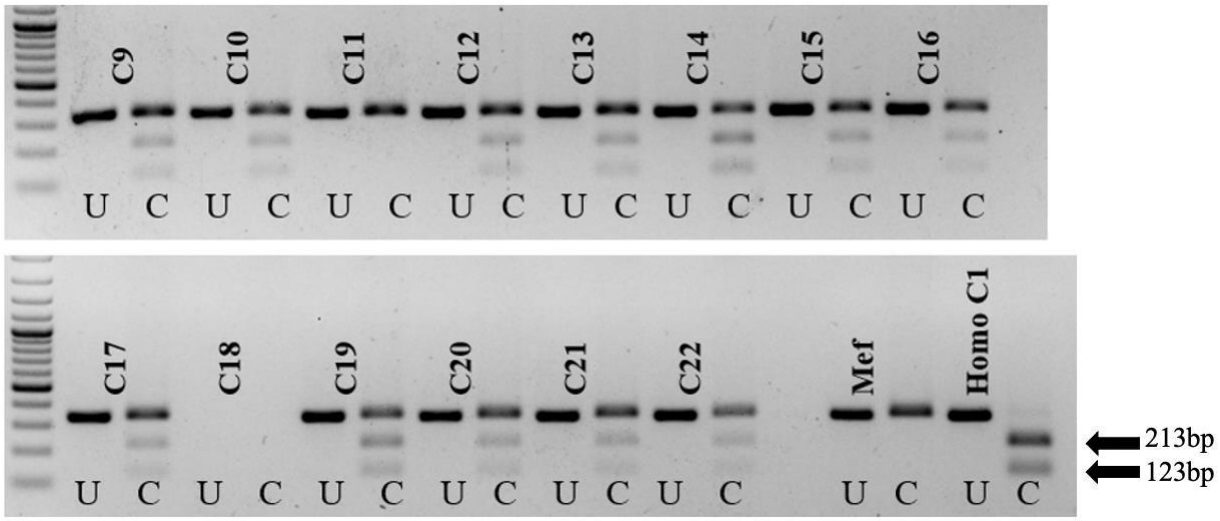

Figure 24. Restriction analysis of live-born second-generation CENP-A edited pups with PstI. Digested products run for 1.5 h at %2 agarose gel with 90V. MEF is used as the negative control, and C1 (knock-in) pup DNA is used for positive control.

4.2.3 CRISPR-edited CENP-A mice

Based on the genotyping results shown in (Figure 21 and 22), we backcrossed C1 and C3 (knock-in females) with C57BL/6 males. Offspring labeled with C9 through C22 have predominantly heterozygous genotypes as expected. Due to the fact that they are born in the same cage, we are unable to distinguish the mothers of the pups (Table 18).

At the (Table 17), we have classified the genotypes of founder mice as WT, knockin or indel. Due to the nature of the CRISP-EZ technique, the genomic editing can take place at different time points during embryo development. Different proportions of cells in the developing embryo might have different genotypes (WT, knockin, insertion, deletion). Due to this genetic mosaicism, it is usually not possible to assign a genotype to the founder mice. We classify these mice as (i) WT when the PCR product is the same size as the WT and does not get digested with the restriction enzyme (PstI), (ii) as knockin when they carry the knockin allele at detectable levels in agarose gel, (iii) as indel when the PCR amplicon is fuzzy or shows bigger or smaller fragments, but restriction digestion does not show the knockin mutation. After founder mice are bred with C57BL/6 mice, the newborns don't have genetic mosaicism. Furthermore, we bred C17 (a heterozygous male) with C12, C13, and C14 (heterozygous females). After pups are born, it will be determined whether a Mendelian distribution will occur.

Table 17. Genotypes of CENP-A knockin founders.

Animal ID	Sex	Generation	Genotype
Cnp-k1 (C1)	F	Founder	Knock-in
Cnp-k2 (C2)	F	Founder	Knock-in
Cnp-k3 (C3)	F	Founder	Knock-in
Cnp-k4 (C4)	F	Founder	WT
Cnp-k5 (C5)	M	Founder	Indel
Cnp-k6 (C6)	M	Founder	Knock-in
Cnp-k7 (C7)	M	Founder	Knock-in
Cnp-k8 (C8)	M	Founder	WT

Table 18. Genotypes of CENP-A new-born pups from backcrossing of C1 and C3 (knockin) females with C57BL/6 males.

Animal ID	Sex	Generation	Genotype
Cnp-k9 (C9)	F	F1N1	Heterozygous
Cnp-k10 (C10)	F	F1N1	Heterozygous
Cnp-k11 (C11)	F	F1N1	WT
Cnp-k12 (C12)	F	F1N1	Heterozygous
Cnp-k13 (C13)	F	F1N1	Heterozygous
Cnp-k14 (C14)	F	F1N1	Heterozygous
Cnp-k15 (C15)	F	F1N1	Heterozygous
Cnp-k16 (C16)	F	F1N1	Heterozygous
Cnp-k17 (C17)	M	F1N1	Heterozygous
Cnp-k19 (C19)	M	F1N1	Heterozygous
Cnp-k20 (C20)	M	F1N1	Heterozygous
Cnp-k21 (C21)	M	F1N1	Heterozygous
Cnp-k22 (C22)	M	F1N1	Heterozygous

5. DISCUSSION

In this study, we aim to create a mouse model that includes mutated S15 and S16 residues at the N-Terminal of CENP-A. We successfully converted targeted S15, and S16 into alanine. There are studies on the N-terminal role of human CENP-A and related PTMs investigation in vitro, particularly in human CENP-A S7p, which is hypothesized to correspond to the mitotic phosphorylation function of mouse CENP-A S15 and S16. (Dalkara, Defne. (2017); Ors et al., 2017). Previous research demonstrated controversial results regarding the role of S7 phosphorylation in centromere function. However, the experiments were carried out generally via using HeLa cells. The fact that CENP-A is a fundamental protein is one of the most difficult aspects of working with it, it's challenging to get rid of completely because CENP-A deficiency is fatal to cells and organisms at the same time very low percentage of the CENP-A amount is sufficient to sustain partial centromere function (Fachinetti et al., 2013). Understanding the CENP-A PTM site function is difficult using in vitro models however, in vivo models will provide more information about the lethality of investigated sites. As another important point, studies that used the siRNA method were biased by partially downregulated CENP-A which may have influenced the results. CENP-A is a highly stable and long-lived protein; as a result, it is challenging to diminish its levels using RNAi technology.

In this research, we were able to create a homozygous mutated CENP-A mouse model which includes S15 and S16 mutated N-Terminal. In our work, we could precisely conclude that blocking phosphorylation at residue serine15 and 16 in the N-terminal of mouse CENP-A is not causing lethal chromosomal abnormality during mitosis. All the mutated mice are perfectly healthy. Despite creating a CENP-A-mutant mouse model for functional research, our results are unable to reveal minor epigenetic modifications arising from S15 and S16 alanine conversion.

This project is based on CRISPR-EZ, which requires correctly designed single-guide RNA (sgRNA). There are limitations to finding PAM sites for desired mutations while sgRNA designing regardless of the source or website you choose. (Cui et al., 2018) Designing and choosing optimized sgRNA for in vivo editing is more challenging because T7 or SP6 promoters in CRISPR/Cas9 system restrict GG or GA in the 5′-end of the sgRNA sequence which resulted in more limited PAM targeting sites. (Moreno-Mateos et al., 2015). In (Figure 14) which is includes

quality confirmation of produced sgRNA for Tyr and CENP-A editing shows the correct size and intact structure of sgRNA. For a better understanding of the sgRNA's quality, we could use a bioanalyzer for the additional control. By using the IVT method for producing sgRNAs, we were able to create mouse models for Tyr and CENP-A. We preferred to use Nested PCR for genotyping because working with embryos (morula-blastocyst stage) is challenging due to their low DNA quantity. (In Figure 17), (Figure 20) and (Figure 23) we were able to get a bold band at the result of two-step PCR. In some embryo screening trials, even nested PCR was unable to amplify target regions. In both Tyr-CENP-A edited embryo genotyping, in some cases, there are bands of slightly different than expected size which is coming from mostly indel mutations. Creating a working genotyping and screening strategy is the key part of the project. According to restriction analysis results in (Figure 18) HinfI (wildtype control), non-digested embryos are also non-digested with EcoRI (HDR-editing control). This may have occurred due to restriction analysis conditions or indel mutations resulting from CRISPR incisions at different locations. This study led to the establishment of a CENP-A mouse model carrying 15S and 16S mutations, as validated by restriction and sequencing analyses.

6. CONCLUSION AND RECOMMENDATIONS

We've achieved two significant findings as a result of the project. Firstly, using the CRISPR-EZ technology, in-vivo models for knock-out and knock-in mutations were successfully produced. In terms of efficacy and simplicity, it is a far superior technique to other in-vivo delivery methods. Secondly, with the phenotypic observation of mutant CENP-A pups, we conclude that the CENP-A S15/S16 mutation is not lethal to the organism. We may further postulate that the conversion of phosphorylation sites (S15/16) to alanine did not lead to abnormal chromosomal segregation. The organism may be able to restore the function of these phosphorylation sites by using other serine or threonine residues in the CENP-A N terminal.

Furthermore, this study requires additional analysis including immunocytochemistry and quantification of mitotic defects for better investigation of possible minor centromere abnormality during the cell cycle. Moreover, despite we observed no lethal phenotype, mutations at S15 and S16 may have resulted in changes in the binding affinity of CENP-A-related substrates, such as CENP-C, CENP-N, and HJURP. In healthy cell division, CENP-A recruits CENP-C and HJURP protein, which helps maintain the CENP-A amount at centromeres. These mutation sites may result in lower CENP-C and HJURP levels, which organisms may be able to tolerate during the cell cycle. At this point, nuclear/mitotic defect analysis should be performed to gain a better understanding of its epigenetic function. In particular, western blotting can be performed to assess changing protein levels during the cell cycle.

In the future perspective, we aim to mutate all serines located in the N-terminal of mouse CENP-A. Creating of such a mouse model will provide a clear picture of the related PTMs and the function of the protein in the cell. In addition, MEF cells derived from mutant CENP-A and WT mice can employ nuclear isolations and immunoblotting methods to obtain a greater understanding of epigenetic modifications.

7. REFERENCES

Allshire, R. C., & Karpen, G. H. (2008). Epigenetic regulation of centromeric chromatin: old dogs, new tricks? Nature Reviews Genetics, 9(12), 923–937. https://doi.org/10.1038/nrg2466

Allshire, R. C., & Madhani, H. D. (2017b). Ten principles of heterochromatin formation and function. Nature Reviews Molecular Cell Biology, 19(4), 229–244. https://doi.org/10.1038/nrm.2017.119

Bailey, A. O., Panchenko, T., Sathyan, K. M., Petkowski, J. J., Pai, P. J., Bai, D. L., Russell, D. H., Macara, I. G., Shabanowitz, J., Hunt, D. F., Black, B. E., & Foltz, D. R. (2013). Posttranslational modification of CENP-A influences the conformation of centromeric chromatin. Proceedings of the National Academy of Sciences, 110(29), 11827–11832. https://doi.org/10.1073/pnas.1300325110

Barra, V., Logsdon, G. A., Scelfo, A., Hoffmann, S., Hervé, S., Aslanian, A., Nechemia-Arbely, Y., Cleveland, D. W., Black, B. E., & Fachinetti, D. (2019a). Phosphorylation of CENP-A on serine 7 does not control centromere function. Nature Communications, 10(1). https://doi.org/10.1038/s41467-018-08073-1

Bodor, D. L., Mata, J. F., Sergeev, M., David, A. F., Salimian, K. J., Panchenko, T., Cleveland, D. W., Black, B. E., Shah, J. V., & Jansen, L. E. (2014). The quantitative architecture of centromeric chromatin. eLife, 3. https://doi.org/10.7554/elife.02137

Caputi, F. F., Candeletti, S., & Romualdi, P. (2017). Epigenetic Approaches in Neuroblastoma Disease Pathogenesis. Neuroblastoma - Current State and Recent Updates. https://doi.org/10.5772/intechopen.69566

Cui, Y., Xu, J., Cheng, M., Liao, X., & Peng, S. (2018). Review of CRISPR/Cas9 sgRNA Design Tools. Interdisciplinary Sciences: Computational Life Sciences, 10(2), 455–465. https://doi.org/10.1007/s12539-018-0298-z

Dalkara, Defne (2017). Epigenetic function of the amino-terminal domain of CENP-A during mitosis. Cellular Biology. Doctorol Thesis Université Grenoble Alpes. NNT: 2017GREAV001 https://tel.archives-ouvertes.fr/tel-02910197/document

de Groot, C., Houston, J., Davis, B., Gerson-Gurwitz, A., Monen, J., Lara-Gonzalez, P., Oegema, K., Shiau, A. K., & Desai, A. (2021). The N-terminal tail of C. elegans CENP-A interacts with KNL-2 and is essential for centromeric chromatin assembly. Molecular Biology of the Cell, 32(12), 1193–1201. https://doi.org/10.1091/mbc.e20-12-0798

Eot-Houllier, G., Magnaghi-Jaulin, L., Fulcrand, G., Moyroud, F. X., Monier, S., & Jaulin, C. (2018). Aurora A-dependent CENP-A phosphorylation at inner centromeres protects bioriented chromosomes against cohesion fatigue. Nature Communications, 9(1). https://doi.org/10.1038/s41467-018-04089-9

Fachinetti, D., Diego Folco, H., Nechemia-Arbely, Y., Valente, L. P., Nguyen, K., Wong, A. J., Zhu, Q., Holland, A. J., Desai, A., Jansen, L. E. T., & Cleveland, D. W. (2013). A two-step mechanism for epigenetic specification of centromere identity and function. Nature Cell Biology, 15(9), 1056–1066. https://doi.org/10.1038/ncb2805

Goutte-Gattat, D., Shuaib, M., Ouararhni, K., Gautier, T., Skoufias, D. A., Hamiche, A., & Dimitrov, S. (2013). Phosphorylation of the CENP-A amino-terminus in mitotic centromeric chromatin is required for kinetochore function. Proceedings of the National Academy of Sciences, 110(21), 8579–8584. https://doi.org/10.1073/pnas.1302955110

Hall, E. C. R., Murgatroyd, C., Stebbings, G. K., Cunniffe, B., Harle, L., Salter, M., Ramadass, A., Westra, J. W., Hunter, E., Akoulitchev, A., & Williams, A. G. (2020). The Prospective Study of Epigenetic Regulatory Profiles in Sport and Exercise Monitored Through Chromosome Conformation Signatures. Genes, 11(8), 905. https://doi.org/10.3390/genes11080905

Hille, F., & Charpentier, E. (2016). CRISPR-Cas: biology, mechanisms and relevance. Philosophical Transactions of the Royal Society B: Biological Sciences, 371(1707), 20150496. https://doi.org/10.1098/rstb.2015.0496

Jansen, L. E., Black, B. E., Foltz, D. R., & Cleveland, D. W. (2007). Propagation of centromeric chromatin requires exit from mitosis. Journal of Cell Biology, 176(6), 795–805. https://doi.org/10.1083/jcb.200701066

Jiang, F., & Doudna, J. A. (2017). CRISPR–Cas9 Structures and Mechanisms. Annual Review of Biophysics, 46(1), 505–529. https://doi.org/10.1146/annurev-biophys-062215-010822

Jinek, M., East, A., Cheng, A., Lin, S., Ma, E., & Doudna, J. (2013). RNA-programmed genome editing in human cells. eLife, 2. https://doi.org/10.7554/elife.00471

Jing, R., Xi, J., Leng, Y., Chen, W., Wang, G., Jia, W., Kang, J., & Zhu, S. (2017). Motifs in the amino-terminus of CENP-A are required for its accumulation within the nucleus and at the centromere. Oncotarget, 8(25), 40654–40667. https://doi.org/10.18632/oncotarget.17204

Khan, F. A., Pandupuspitasari, N. S., Chun-Jie, H., Ao, Z., Jamal, M., Zohaib, A., Khan, F. A., Hakim, M. R., & ShuJun, Z. (2016). CRISPR/Cas9 therapeutics: a cure for cancer and other genetic diseases. Oncotarget, 7(32), 52541–52552. https://doi.org/10.18632/oncotarget.9646

Kunitoku, N., Sasayama, T., Marumoto, T., Zhang, D., Honda, S., Kobayashi, O., Hatakeyama, K., Ushio, Y., Saya, H., & Hirota, T. (2003). CENP-A Phosphorylation by Aurora-A in Prophase Is Required for Enrichment of Aurora-B at Inner Centromeres and for Kinetochore Function. Developmental Cell, 5(6), 853–864. https://doi.org/10.1016/s1534-5807(03)00364-2

Lee, J., & Orr-Weaver, T. (2001). Chromatin. Encyclopedia of Genetics, 340–343. https://doi.org/10.1006/rwgn.2001.0199

Mariño-Ramírez, L., Kann, M. G., Shoemaker, B. A., & Landsman, D. (2005). Histone structure and nucleosome stability. Expert Review of Proteomics, 2(5), 719–729. https://doi.org/10.1586/14789450.2.5.719

McKinley, K. L., & Cheeseman, I. M. (2015). The molecular basis for centromere identity and function. Nature Reviews Molecular Cell Biology, 17(1), 16–29. https://doi.org/10.1038/nrm.2015.5

Modzelewski, A. J., Chen, S., Willis, B. J., Lloyd, K. C. K., Wood, J. A., & He, L. (2018). Efficient mouse genome engineering by CRISPR-EZ technology. Nature Protocols, 13(6), 1253–1274. https://doi.org/10.1038/nprot.2018.012

Moreno-Mateos, M. A., Vejnar, C. E., Beaudoin, J. D., Fernandez, J. P., Mis, E. K., Khokha, M. K., & Giraldez, A. J. (2015). CRISPRscan: designing highly efficient sgRNAs for CRISPR-Cas9 targeting in vivo. Nature Methods, 12(10), 982–988. https://doi.org/10.1038/nmeth.3543

Morrison, O., & Thakur, J. (2021). Molecular Complexes at Euchromatin, Heterochromatin and Centromeric Chromatin. International Journal of Molecular Sciences, 22(13), 6922. https://doi.org/10.3390/ijms22136922

Müller, S., & Almouzni, G. (2017). Chromatin dynamics during the cell cycle at centromeres. Nature Reviews Genetics, 18(3), 192–208. https://doi.org/10.1038/nrg.2016.157

Ors, A., Papin, C., Favier, B., Roulland, Y., Dalkara, D., Ozturk, M., Hamiche, A., Dimitrov, S., & Padmanabhan, K. (2017). Histone H3.3 regulates mitotic progression in mouse embryonic fibroblasts. Biochemistry and Cell Biology, 95(4), 491–499. https://doi.org/10.1139/bcb-2016-0190

Ramazi, S., Allahverdi, A., & Zahiri, J. (2020). Evaluation of post-translational modifications in histone proteins: A review on histone modification defects in developmental and neurological disorders. Journal of Biosciences, 45(1). https://doi.org/10.1007/s12038-020-00099-2

Richardson, C. D., Ray, G. J., DeWitt, M. A., Curie, G. L., & Corn, J. E. (2016). Enhancing homology-directed genome editing by catalytically active and inactive CRISPR-Cas9 using asymmetric donor DNA. Nature Biotechnology, 34(3), 339–344. https://doi.org/10.1038/nbt.3481

Rossetto, D., Avvakumov, N., & Côté, J. (2012). Histone phosphorylation. Epigenetics, 7(10), 1098–1108. https://doi.org/10.4161/epi.21975

Sathyan, K. M., Fachinetti, D., & Foltz, D. R. (2017). α-amino trimethylation of CENP-A by NRMT is required for full recruitment of the centromere. Nature Communications, 8(1). https://doi.org/10.1038/ncomms14678

Shalaby, K., Aouida, M., & El-Agnaf, O. (2020). Tissue-Specific Delivery of CRISPR Therapeutics: Strategies and Mechanisms of Non-Viral Vectors. International Journal of Molecular Sciences, 21(19), 7353. https://doi.org/10.3390/ijms21197353

Sharma, A., Singh, K., & Almasan, A. (2012). Histone H2AX Phosphorylation: A Marker for DNA Damage. Methods in Molecular Biology, 613–626. https://doi.org/10.1007/978-1-61779-998-3_40

Shuaib, M., Ouararhni, K., Dimitrov, S., & Hamiche, A. (2010). HJURP binds CENP-A via a highly conserved N-terminal domain and mediates its deposition at centromeres. Proceedings of the National Academy of Sciences, 107(4), 1349–1354. https://doi.org/10.1073/pnas.0913709107

Silva, M., Bodor, D., Stellfox, M., Martins, N., Hochegger, H., Foltz, D., & Jansen, L. (2012). Cdk Activity Couples Epigenetic Centromere Inheritance to Cell Cycle Progression. Developmental Cell, 22(1), 52–63. https://doi.org/10.1016/j.devcel.2011.10.014

Sitbon, D., Podsypanina, K., Yadav, T., & Almouzni, G. (2017). Shaping Chromatin in the Nucleus: The Bricks and the Architects. Cold Spring Harbor Symposia on Quantitative Biology, 82, 1–14. https://doi.org/10.1101/sqb.2017.82.033753

Strahl, B. D., & Allis, C. D. (2000). The language of covalent histone modifications. Nature, 403(6765), 41–45. https://doi.org/10.1038/47412

Szenker, E., Ray-Gallet, D., & Almouzni, G. (2011). The double face of the histone variant H3.3. Cell Research, 21(3), 421–434. https://doi.org/10.1038/cr.2011.14

Tachiwana, H., Kagawa, W., Shiga, T., Osakabe, A., Miya, Y., Saito, K., Hayashi-Takanaka, Y., Oda, T., Sato, M., Park, S. Y., Kimura, H., & Kurumizaka, H. (2011). Crystal structure of the human centromeric nucleosome containing CENP-A. Nature, 476(7359), 232–235. https://doi.org/10.1038/nature10258

Takada, M., Zhang, W., Suzuki, A., Kuroda, T. S., Yu, Z., Inuzuka, H., Gao, D., Wan, L., Zhuang, M., Hu, L., Zhai, B., Fry, C. J., Bloom, K., Li, G., Karpen, G. H., Wei, W., &

Zhang, Q. (2017a). FBW7 Loss Promotes Chromosomal Instability and Tumorigenesis via Cyclin E1/CDK2–Mediated Phosphorylation of CENP-A. Cancer Research, 77(18), 4881–4893. https://doi.org/10.1158/0008-5472.can-17-1240

Talbert, P. B., & Henikoff, S. (2021). Histone variants at a glance. Journal of Cell Science, 134(6). https://doi.org/10.1242/jcs.244749

Truett, G., Heeger, P., Mynatt, R., Truett, A., Walker, J., & Warman, M. (2000). Preparation of PCR-Quality Mouse Genomic DNA with Hot Sodium Hydroxide and Tris (HotSHOT). BioTechniques, 29(1), 52–54. https://doi.org/10.2144/00291bm09

Woodcock, C. L., & Dimitrov, S. (2001). Higher-order structure of chromatin and chromosomes. Current Opinion in Genetics & Development, 11(2), 130–135. https://doi.org/10.1016/s0959-437x(00)00169-6

Zeitlin, S. G., Shelby, R. D., & Sullivan, K. F. (2001). CENP-A is phosphorylated by Aurora B kinase and plays an unexpected role in completion of cytokinesis. Journal of Cell Biology, 155(7), 1147–1158. https://doi.org/10.1083/jcb.200108125

8. APPENDIX

8.1 Curriculum Vitae

Tuğba Şehitoğulları

Year of Birth	
Address:	İ
Telephone:	
Fax:	
e-mail:	

EDUCATION

Country	University	Faculty/Institute	Field	Degree	Year of Graduation
TR	Dokuz Eylul University	İzmir International Biomedicine and Genome Institute	Molecular Biology and Genetics	M.Sc.	2022
TR	Acıbadem University	Faculty of Science	Molecular Biology and Genetics	B.Sc.	2020

AKADEMIC EXPERIENCE

Institution	Country	Laboratory	Department	Title
Izmir Biomedicine and Genome Center	Turkey	Prof. Dr. Mehmet ÖZTÜRK	Molecular Biology and Genetics	Intern
Acıbadem University	Turkey	Prof. Uğur SEZERMAN	Bioinformatics	Intern
Vrije-Amsterdam University	Holland	Summer Internship Program	Molecular Biology and Genetics	Intern
Nagasaki University	Japan	Prof. Dr. Koyo NİSHİDA	Biomedical Sciences	Intern
Acıbadem University	Turkey	Asst. Prof. Zeynep Tokçaer KESKİN	Molecular Biology and Genetics	Intern

RESEARCH FIELDS

Life Sciences

Publications or statements in the proceedings of refereed conferences/symposiums.

Generation of transgenic mouse models from zygote stage embryos by CRISPR genome engineering. XVII. MEDICAL BIOLOGY AND GENETICS CONGRESS in Turkey.

8.2. Ethics Committee Approval

İZMİR BİYOTIP VE GENOM MERKEZİ
HAYVAN DENEYLERİ YEREL ETİK KURULU (İBG-HADYEK)
KARARI

Toplantı Tarihi	: 16/02/2022	**Toplantı Günü**	: Çarşamba
Toplantı Sayısı	: 4	**Toplantı Saati**	: 15:30

Sayın Doç. Dr. Muhammed Kasım DIRIL,

2022-004 Protokol No'lu; yürütücüsü olduğunuz "CENP-A amino terminalinin epigenetik fonksiyonlarının in vivo incelenmesi" başlıklı projenin uygulanmasında etik açıdan sakınca olmadığına oy birliği ile karar verilmiştir.

Bilgilerinizi ve gereğini rica ederiz.

Dr. Gülçin ÇAKAN AKDOĞAN **Başkan**	(Projede Araştırmacı) **Vet. Hek. Kerem ESMEN** **Başkan Yardımcısı**
Prof. Dr. Ensari GÜNELİ **Üye**	**Doç. Dr. Güneş ÖZHAN** **Üye**
(Proje Yürütücüsü) **Doç. Dr. Kasım DİRİL** **Üye**	**Dr. Yavuz DOĞAN** **Üye**
Vet. Hek. Umur KELEŞ **Üye**	**Vet. Hek. Ceren ÜLKER** **Üye**
Vet. Hek. Gizem ARALAN **Üye**	**İrem KARADAŞ** **Üye**